

DESIGN OF AN OFFSET FED SCANNING
ANTENNA FOR THE SHUTTLE IMAGING
MICROWAVE SYSTEM

14 April 1975

No. TR070
Interim Report
JPL Contract No. 954145

NAS7-100

Prepared for
JET PROPULSION LABORATORY
CALIFORNIA INSTITUTE OF TECHNOLOGY



(NASA-CR-147166) DESIGN OF AN OFFSET FED	N76-22287
SCANNING ANTENNA FOR THE SHUTTLE IMAGING	
MICROWAVE SYSTEM Interim Report (Gustincic	
(J. J.) Consulting Engineer) 64 p HC \$4.50	Unclas
CSCS 09C G3/19	26816

Prepared by

J.J. Gustincic
Consulting Engineer
13121 Mindanao Way
Marina Del Rey, CA
90291

DESIGN OF AN OFFSET FED SCANNING ANTENNA FOR
THE SHUTTLE IMAGING MICROWAVE SYSTEM

Report No TR070
Interim Report
JPL Contract No 954145

Prepared for
JET PROPULSION LABORATORY
California Institute of Technology
4800 Oak Grove Drive
Pasadena, California 91103

Prepared by
J J Gustincic
Consulting Engineer
13121 Mindanao Way
Marina Del Rey, California 90291

14 April 1975

This work was performed for the Jet Propulsion Laboratory,
California Institute of Technology, sponsored by the
National Aeronautics and Space Administration under
Contract NAS7-100

This report contains information prepared by
J J Gustincic under JPL subcontract Its content is
not necessarily endorsed by the Jet Propulsion Laboratory,
California Institute of Technology, or the National
Aeronautics and Space Administration

ABSTRACT

This report describes a design study for a mechanically scanned offset fed parabolic torus reflector antenna having a 4m x 2m aperture for simultaneous use at eleven frequency channels from UHF to millimeter wavelengths. A design for the antenna is presented utilizing dipole and horn feeds at the low frequencies and a Gregorian aberration correcting subreflector system for feeding the torus at the high frequencies. The results and details of a theoretical study based on geometrical optics performed to evaluate the high frequency design and the results of an experimental study involving a one-tenth scale model for evaluation of the low-frequency behavior are given. Beam efficiencies, antenna patterns, beamwidths and cross polarization levels are presented and these results demonstrate that the antenna concept is viable for the Shuttle Imaging Microwave System requirement.

TABLE OF CONTENTS

1 0	SUMMARY AND INTRODUCTION	1
1 1	Purpose and Scope	1
1 2	Study Description	4
1 2 1	High Frequency Performance	4
1 2 2	Low Frequency Performance	5
1 3	Summary of Results	6
2 0	HIGH FREQUENCY STUDY	9
2 1	Antenna Design Procedure	9
2 1 1	Energy Transformation Mapping	10
2 1 2	Cross Polarization Mapping	13
2 2	Final Design and Evaluation	16
2 2 1	Calculated Electrical Performance	19
3 0	LOW FREQUENCY STUDY	25
3 1	Engineering Performance Estimates	25
3 1 1	Path Length Error	25
3 1 2	Cross Polarization	29
3 2	Scale Model	29
3 2 1	Model Description	29
3 2 2	Model Feed	31
3 3 3	Model Measurements	32
4 0	ANALYSES	40
4 1	Geometrical Optics Analysis	40
4 2	Low Frequency Analysis	51
5 0	CONCLUSIONS AND RECOMMENDATIONS	56
6 0	NEW TECHNOLOGY	56
7 0	REFERENCES	57
8 0	APPENDIX A	58

1 0 SUMMARY AND INTRODUCTION

1 1 Purpose and Scope

This report describes the results of a three-man month study undertaken to obtain design for an offset fed reflector scanning system which will meet the electrical requirements of the Shuttle Imaging Microwave System (SIMS). Basically, the SIMS antenna system requires a high efficiency, dual polarized, wide angle scanning antenna, operating simultaneously at eleven frequencies distributed over the entire microwave spectrum. The significant electrical performance requirements and size limitations for the SIMS antenna are summarized in Table I.

TABLE I
SIMS Antenna Requirements

Polarization	Dual Orthogonal Linear
Beam Efficiency	$\geq 90\%$
Radiating Aperture Diameter	$\sim 2\text{m}$
Scan Range	$\pm 60^\circ$ from Nadir in cross-track plane
Size	4m x 3m x 3m
Frequencies and Bandwidths	

<u>Frequency (GHZ)</u>	<u>Bandwidth (MHZ)</u>
118.7	700
94.0	2000
53.0	500
37.0	2000
22.2	1000
20.0	1000
10.69	300
6.6	300
2.695	10
1.413	25
610	8

A mechanically scanned antenna system consisting of a parabolic torus reflector offset fed by a large number of feeds mounted on a rotating feed wheel was suggested for the SIMS requirement in a previous study ⁽¹⁾ This antenna scheme is the object of this report and is illustrated in Fig 1 As seen in the figure, as the feed support wheel turns various feeds move around the reflector feed locus producing multiple synchronus scanning beams

At about 10.69 GHz and above the illuminated portion of the torus reflector deviates sufficiently from a true parabola so that a feed system must be employed which can correct the aberrations produced by the torus At lower frequencies the aberration is relatively unimportant or easily corrected and simple radiators suitable for the illumination of parabolic reflectors can be positioned to give acceptable performance

Two typical feeds are shown in Fig 1, a dipole array suitable for generating the reflector illumination at the lowest frequencies and a Gregorian subreflector system, which is capable of feeding the reflector properly at the highest frequencies where aberration corrections are required These two feeds are representative of all the feeds required to generate the eleven SIMS frequencies and therefore the design and performance of the antenna with these two feed systems was the major objective of this study

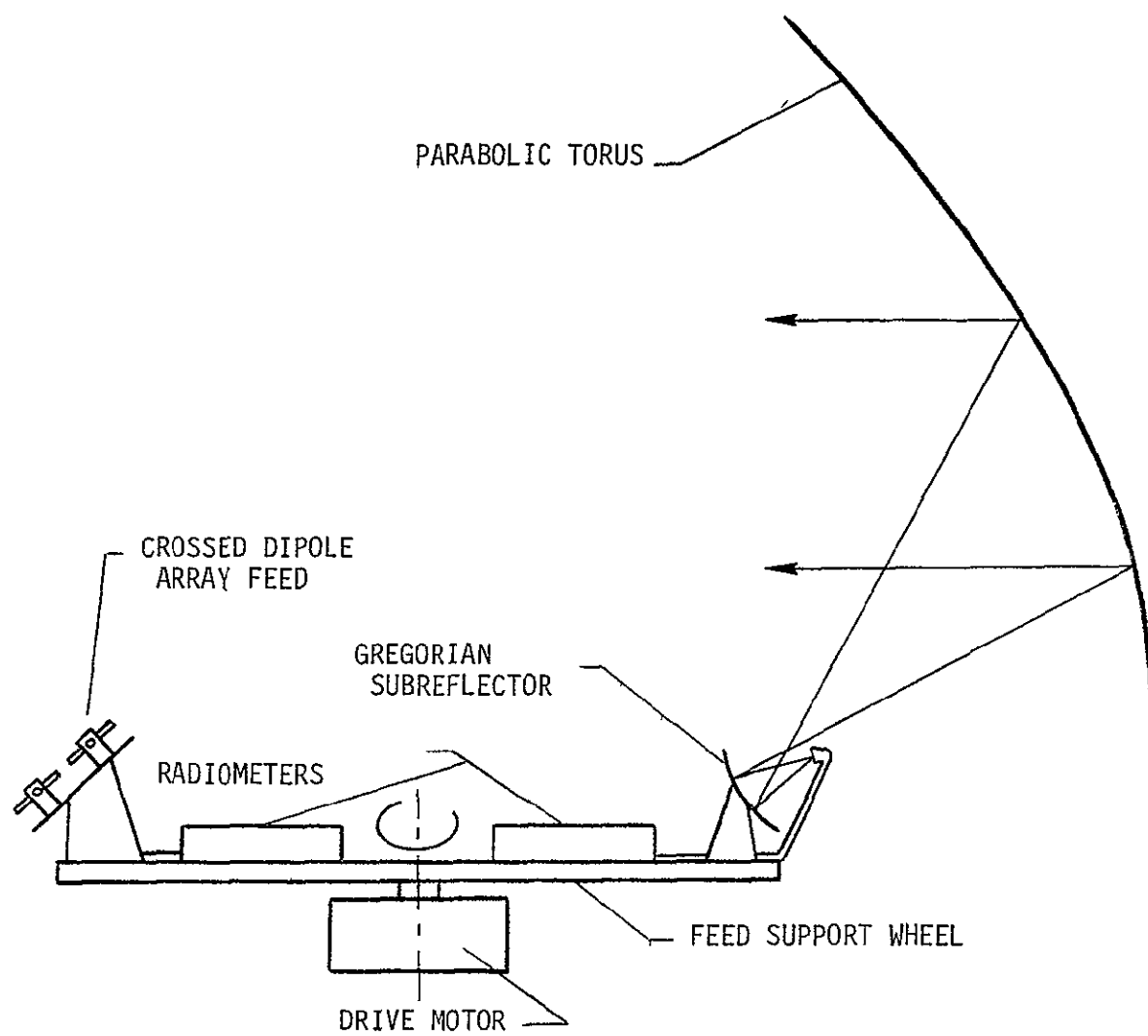


FIG 1 The offset fed SIMS antenna

1 2 Study Description

1 2 1 High Frequency Performance

The high frequency antenna design and performance evaluation was accomplished by a theoretical computation based on geometrical optics. A computer program was written to determine the coordinates of the Gregorian subreflector for a given choice of feed and subreflector position. The antenna aperture distribution was then computed on the basis of geometrical optics and an assumed typical Gaussian beam shape from the feed horn which illuminates the subreflector. The cross polarized aperture illumination was also calculated by taking into account the physical optics current induced on the curved torus reflector and Gregorian subreflector. By comparing the total amount of cross polarized power crossing the antenna aperture to the power crossing the aperture in the principal polarization, the cross polarization level of the antenna was determined. The far field antenna patterns were then computed from the calculated aperture distribution for the principal polarization and the patterns numerically integrated to yield the antenna beam efficiency. By its very nature the geometrical optics analysis did not treat the effects of spillover past the region of reflector illumination.

By making repeated use of this computer program an antenna design study was performed to simultaneously optimize the antenna beam efficiency, cross polarization, beamwidths and subreflector size, and spillover by determining the best choice for the following antenna design parameters

- 1) Subreflector Position
- 2) Feed Position

- 3) Feed Beamwidths
- 4) Feed Pointing Angle
- 5) Region of Reflector Illumination

The high frequency study is described in detail in Section 2.0 of this report

1.2.2 Low Frequency Performance

At the very low frequencies of operation it is difficult to make a meaningful calculation of the antenna performance inasmuch as the reflector is only a few wavelengths in height and such effects as feed backlobes, spillover and blockage produced by the projection of the feed wheel are not directly tractable. An experimental study was therefore performed to predict the antenna performance at 610 GHz. A nearly one-tenth scale model of the antenna was designed, fabricated and measured at 6.52 GHz. The model utilized a four dipole array feed and antenna patterns were measured in the two principal planes and the diagonal plane. The patterns were integrated to give values for beam efficiency and cross polarization.

Some additional engineering estimates of the low frequency antenna performance were also obtained by calculating the path length phase error which results when a simple point source feed is placed at certain optimum positions around the torus feed locus. Cross polarization levels due to reflector curvature were also estimated for the low frequency case.

The low frequency study is contained in Section 3.0

1 3 Summary of Results

A quantitative summary of the electrical performance of the antenna system at the highest and lowest frequencies of operation as predicted by the theoretical and experimental work described in detail in the remainder of this report is presented in Table I-A. These results generally indicate that the offset parabolic torus antenna scheme is a viable and sound method for satisfying the SIMS requirements. The table shows the required high beam efficiencies along with beamwidths consistent with a reasonable use of a 2m diameter aperture. The table also indicates that the total amount of received cross polarized power due to reflector curvature effects is in the order of a few percent. The circular symmetry of the geometry ensures satisfactory operation over the required scan range.

The engineering estimates of Section 3.0 show that any simple radiator such as a horn or dipole array with a circular beam having a 3 dB width of 45° can be used to satisfactorily illuminate the torus at the low frequencies up to and including 2.695 GHz. The use of such radiators results in a beam squint up from the plane of the feed wheel of about 5° . At 6.6 GHz some aberration correction of the simple feed may be required.

At 10.69 GHz the subreflector has a minimum dimension of 10 wavelengths. Thus, the subreflectors should be useable at this frequency and above. The subreflectors are of such a dimension that eight of them can be placed around the periphery of the feed wheel in addition to the feeds required for the low frequencies. By utilizing multiple frequency clustered horns to feed the subreflectors, the system has a

TABLE I-A

Electrical Performance Summary - 4m Diameter Torus

Frequency	118.7 GHz	610 GHz
Evaluation Method	Geometrical Optics Analysis	6.5 GHz Scale Model Measurements
Feed Type	Gregorian Subreflector Simple Horn	4 Dipole Array
Feed Dimensions	31cm x 56cm	54cm x 54cm
Beam Efficiency (Excluding Cross Polarization)	91%	95%
Track Plane 3 dB Beamwidth	110°	19°
Scan Plane 3 dB Beamwidth	103°	16°
Diagonal Plane 3 dB Beamwidth	101°	18°
Integrated Fractional Cross Polarized Power		
Vertically Polarized Feed	3.2%	3.8%
Horizontally Polarized Feed	1.8%	4.3%
		(computed)

channel capability greatly exceeding the requirements of Table I in both number and bandwidth. The total antenna volume will be approximately $4\text{m} \times 2.5\text{m} \times 3\text{m}$, satisfying the size allocation requirement.

2 0 HIGH FREQUENCY STUDY

2 1 Antenna Design Procedure

In this section the procedure utilized for obtaining a specific high frequency subreflector-feed design is described. The torus reflector and subreflector feed system exhibits primarily two effects detrimental to the generation of a high beam efficiency antenna pattern. The first effect is the generation of cross polarization due to the curvature of the reflector surfaces. Certain regions of the torus are exceedingly curved and their illumination results in severe cross polarization. The second undesirable effect is due to the fact that in those regions where the torus begins to deviate appreciably from a true parabola, the ray bundles from the reflector begin to diverge drastically. This happens in such a way that a given increment of area on the aperture plane is illuminated by a disproportionately large area of the subreflector. The large subreflector area collects more than its share of energy from the feed horn and thus there is a tendency of the feed horn energy to be focussed into "hot spots" at the edges of the aperture where the aberration is greatest. This energy transformation effect prevents the establishment of a smoothly tapered amplitude distribution. This effect and the effect of cross polarization generation must be minimized by the appropriate choice of subreflector-feed horn design as will now be discussed.

Due to the transcendental nature of the required analysis the antenna design study was performed by a purely numerical technique. A computer program was written to predict the subreflector shape and aperture fields for a given choice of subreflector position and feed characteristics. The details of the analysis and definitions of the

design parameters are presented in the geometrical optics analysis of Section 4.1. The resulting FORTRAN computer code is included in Appendix A labeled as program MAIN. The radiating aperture plane was taken to be the X-Z plane with the Z-axis corresponding to the axis of the wheel and the X-axis perpendicular to the antenna beam pointing direction. The first quadrant of the aperture plane was covered by a grid of 66 points as shown in Fig. 2. Program MAIN was then used to calculate the antenna characteristics for rays passing through each of the grid points. Maps of the aperture characteristics were then made at the grid points and the maps were used to determine which regions of the torus reflector were the most suitable for illumination. The antenna exhibits a symmetry about the Z-axis so only the first quadrant of the X-Z plane was investigated. The mapping techniques are discussed in the following sections.

2.1.1 Energy Transformation Mapping

Fig. 3 illustrates how the energy from the feed is transformed to the antenna aperture. A bundle of rays terminating at an area element, S_0 at the point X, Z in the antenna aperture originate from an area $\vec{S}_1(X, Z)$ on the subreflector. If $\vec{RR}(X, Z)$ is the vector from the feed-horn to \vec{S}_1 then, noting that the feed power falls off as $|\vec{RR}|^{-2}$, the relative power density at S_0 is then

$$P(X, Z) = T(X, Z) G(\vec{RR})$$

where $G(\vec{RR})$ is the gain of the feed in the direction of \vec{RR} and the energy transformation T is

$$T = \frac{\vec{S}_1 \cdot \vec{RR}}{S_0 |\vec{RR}|^3}$$

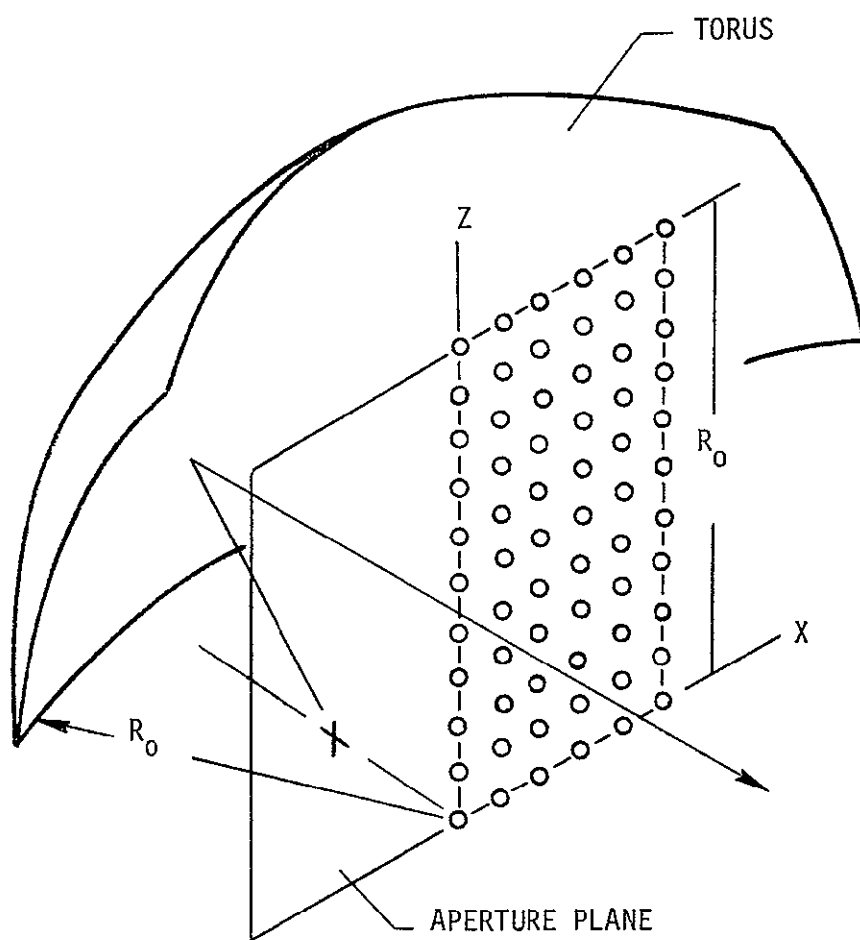


FIG 2 Aperture plane grid

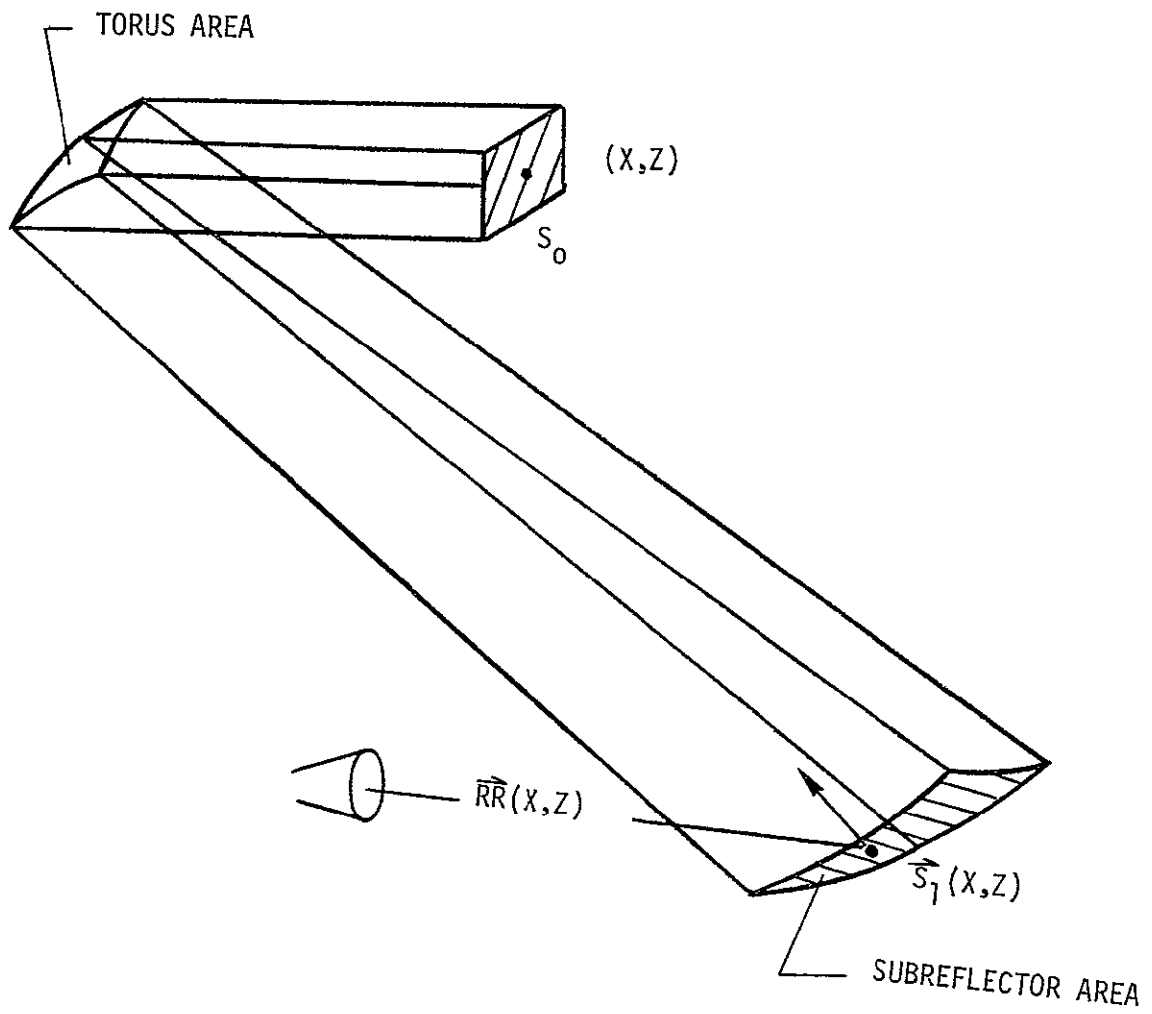


FIG 3 Feed power density transformation

The transformation T then determines how the feed pattern is amplified into the antenna aperture. Fig. 4 shows a typical T map of the aperture as calculated from program MAIN. The grid spacing is 0.1, normalized to the radius of the base of the torus. The transformation has been normalized to unity at the center of the region of least aberration, i.e., $X = 0$, $Z = 0$. It is seen that T becomes very large in the upper right hand corner and along the line $X = 0.5$. A value of $T = 10$, for example, would imply that a -10 dB feed illumination of the subreflector would exhibit itself as a 0 dB illumination in the aperture plane. Clearly these regions are unacceptable for use in this high beam efficiency application.

2.1.2 Cross Polarization Mapping

The computer program MAIN calculates the ratio of cross polarized field to principally polarized field in the antenna aperture. This cross polarization ratio is labeled as CPRV for a vertically polarized feed and CPRH for a horizontally polarized feed. The calculation assumes a physical optics behavior for the reflector currents and a feed horn magnetic field in the same direction as the magnetic field of an elementary linearly polarized current element. A typical aperture map of the cross polarization ratio CPRV is shown in Fig. 5. It can be seen that the cross polarization is extremely large at the top of the reflector. Thus, some care must be taken in the selection of the height of the illuminated region of the reflector.

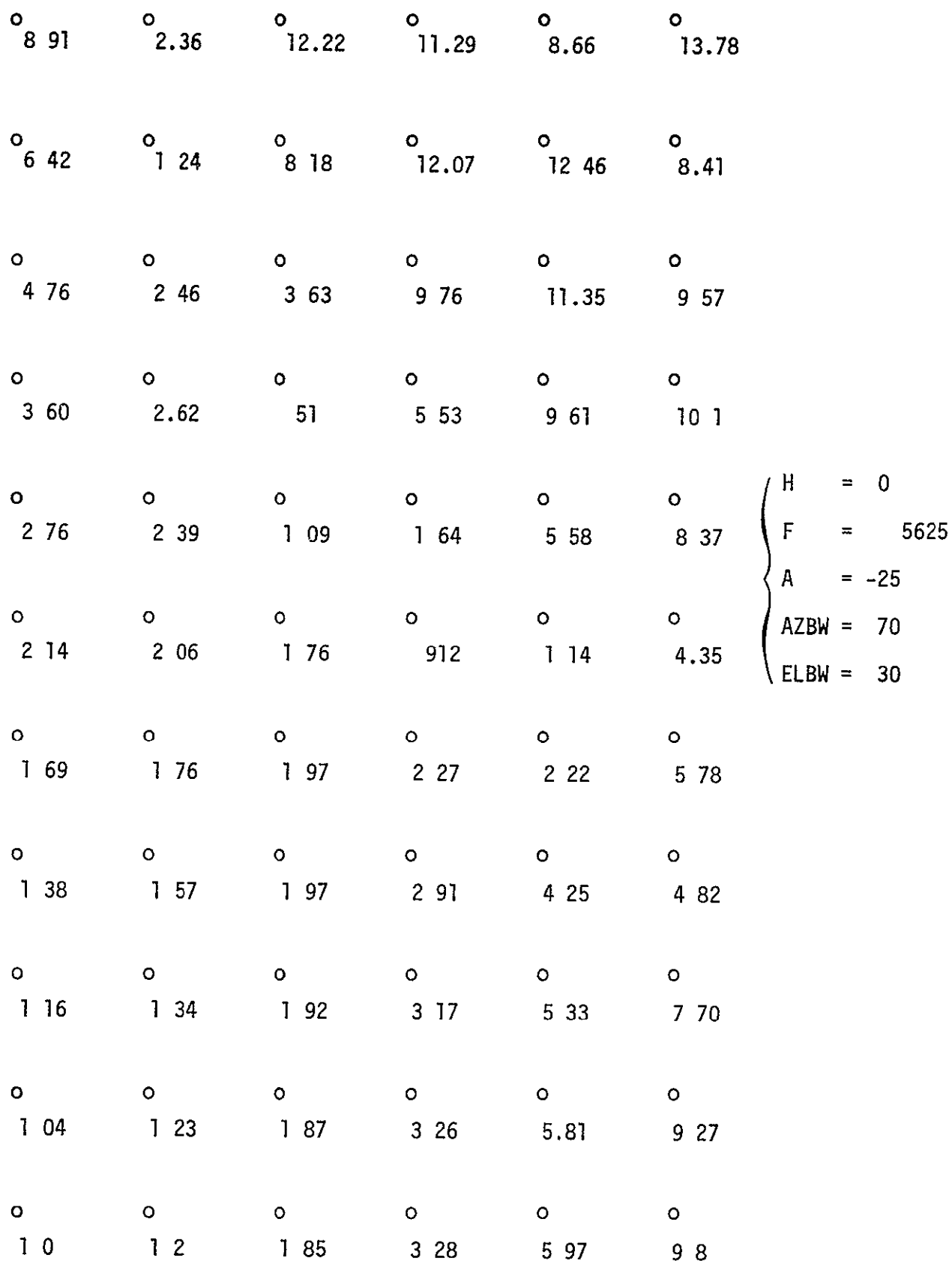


FIG 4 Typical T map

0.	1 60	4.41	5.94	3.10	1.03
0	870	2 15	3.70	3 63	2.29
0	496	1 18	2 16	2 93	2 61
0	.28	66	1 20	1 96	2 29
0	16	37	70	1 18	1 66
0.	09	19	37	.66	1 05
0	04	10	18	34	60
0	02	04	08	15	28
0	01	01	02	03	08
0	00	01	02	04	0.06
0	01	02	.05	11	19

$$\text{CPRV} = \frac{E_x}{E_y}$$

$$\begin{aligned} H &= 04 \\ F &= 5625 \\ S &= 4375 \\ A &= -10 \\ \text{AZBW} &= 70 \\ \text{ELBW} &= 30 \end{aligned}$$

FIG 5 Typical values of the cross polarization ratio CPRV

2.2 Final Antenna Design and Evaluation

In addition to the aperture maps previously discussed the program MAIN was used to generate the principally polarized aperture fields and these fields were numerically integrated to generate far field antenna patterns. The total cross polarized power crossing the antenna aperture was also obtained by numerical integration and compared to the total principally polarized power. After a thorough comparison of the aperture maps, cross polarization levels, and secondary patterns for about 20 choices of feed position and subreflector placement, a final antenna design was selected which appeared to give the best all around optimization of the antenna characteristics. In terms of the design parameters defined in Table II of Section 4.1 the optimum parameter choice occurred for

$$H = 0.813$$

$$F = 5625$$

$$S = 40$$

$$A = 0$$

$$AZBW = 60$$

$$ELBW = 30$$

The study was made for subreflector positions within a tenth of the torus radius from the paraxial focus and feed depressions up to one-tenth the torus radius, i.e.,

$$4 \leq S \leq 5$$

$$0 \leq H \leq 1$$

The restrictions on the maximum value of S and H were necessary to limit the size of the subreflector to a reasonable value. The feed displacement toward the subreflector strongly influenced the angles which the subreflector subtends at the feed. Feed positions were chosen such as to limit the 3 dB widths of the feed to the range of 20° to 70° so that simple horn illuminators could be used. This restricted the range of feed displacements to roughly $55 \leq F \leq 60$.

The antenna design and calculated performance will now be described. The selected portion of the reflector most suitable for illumination is the region within the dashed lines shown in Fig. 6. Noting that the grid spacing is 0.1, normalized to the radius of the base of the torus, it can be seen that the illuminated region has a width and height of 80% of the torus radius. This reasonably small reduction of the available aperture is the compromise required to ensure high beam efficiency and low cross polarization at the higher frequencies. Because the torus reflector curves inward, the maximum dimension of the antenna will be less than twice the torus radius, $2R_0$. For the illuminated region of Fig. 6, and a 120° total scan range, an examination of the geometry reveals that the torus diameter is 2.5% greater than the maximum dimension of the antenna thus effectively making the 20% aperture reduction only 17.5%. Furthermore, if the elimination of a very small area in the lower right hand corner of the illuminated region of Fig. 6 can be tolerated at the limits of the range of scan, a 10% increase in resolution should easily be possible. A reduction in the scan range would also allow an increase in $2R_0$ for a fixed antenna dimension.

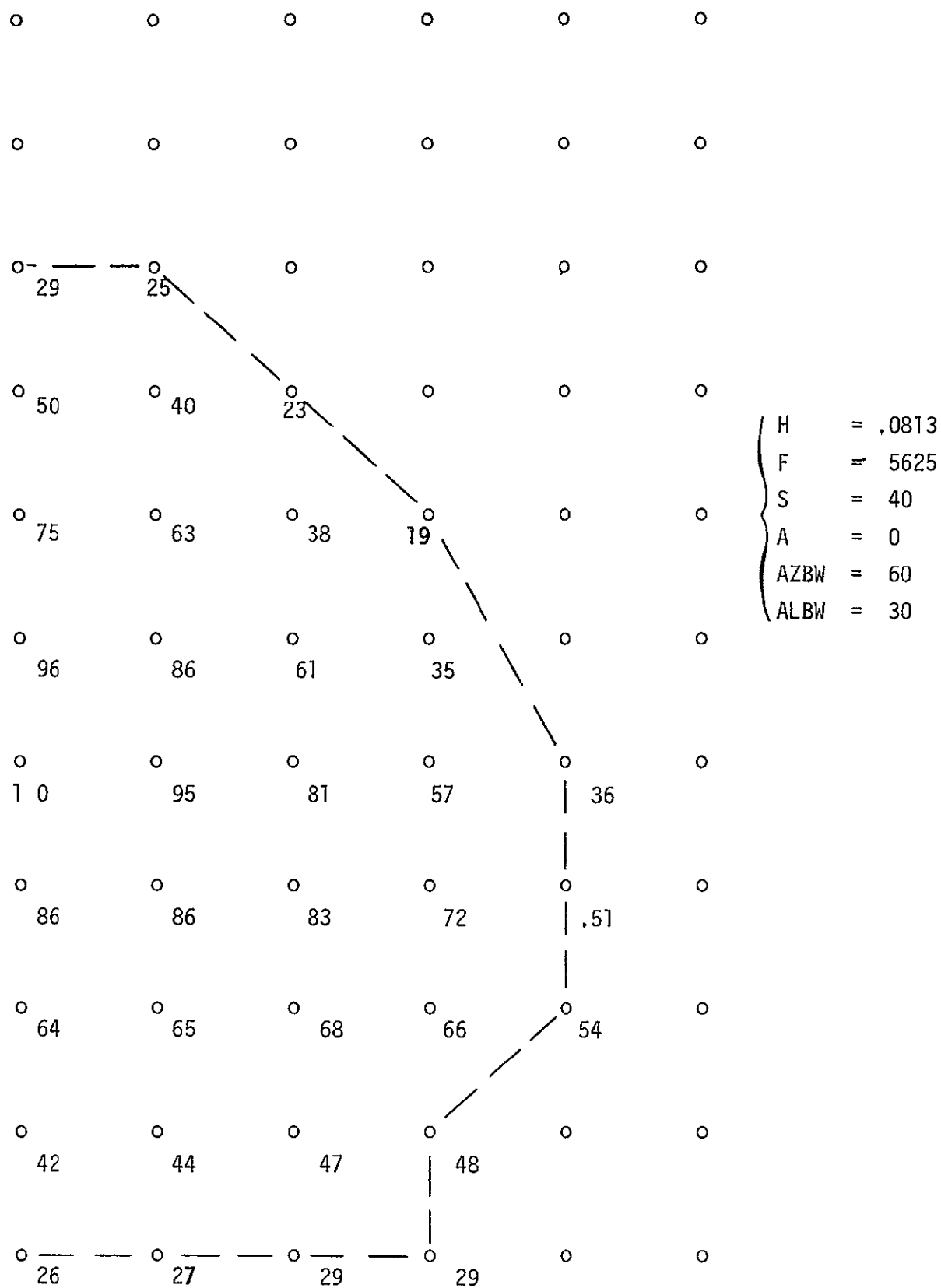


FIG 6 Aperture illumination

The narrowest secondary beams consistent with acceptable subreflector spillover levels occur when the feed horn has elevation and azimuth 3 dB beamwidths of 30° and 60° , respectively. For this feed choice the subreflector spillover which will be absorbed by absorbing material around the subreflector periphery is less than 0.5 dB. The principally polarized aperture field distribution which results from this feed pattern is also shown at the grid points in Fig. 6. The illumination decreases smoothly from the center of the aperture to an average edge taper of about 10 dB.

The subreflector and horn geometry for this design is shown in the scale drawing of Fig. 7 along with their positions relative to the paraxial focal point at 0, 5, 0. The subreflector has a dimension of roughly 2' by 1'. Approximately ten such subreflectors could be put around the feed wheel periphery. The coordinates of the subreflector are calculated by program MAIN in Appendix A.

2.2.1 Calculated Electrical Performance

By integrating the square of the computed aperture fields over the aperture, the total cross polarized power crossing the aperture was calculated as a fraction of the total principally polarized power. This ratio was found to be 3.2% for a vertically polarized feed, and 1.9% for a horizontally polarized feed.

The calculated secondary patterns for the antenna for the principal and diagonal planes are shown in Figs. 8, 9 and 10. The angular scales on these patterns are not labeled as only the shape of the patterns

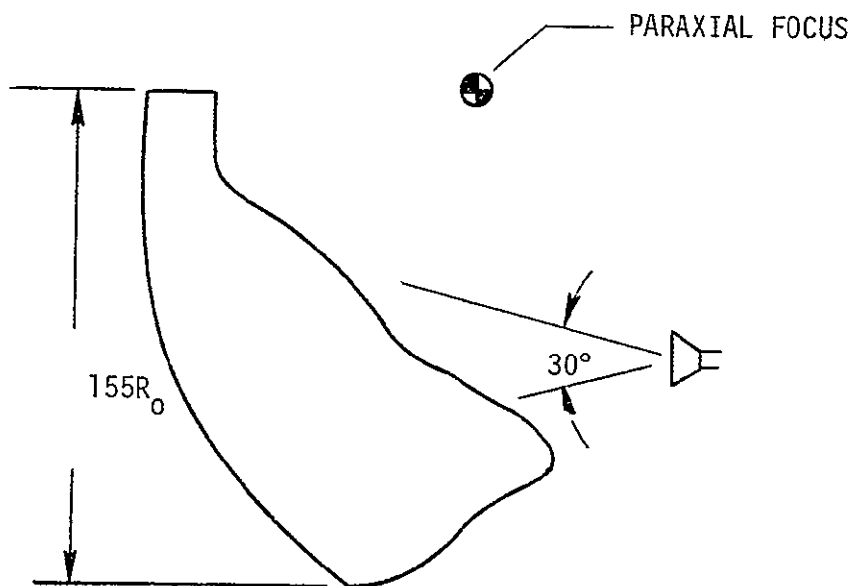
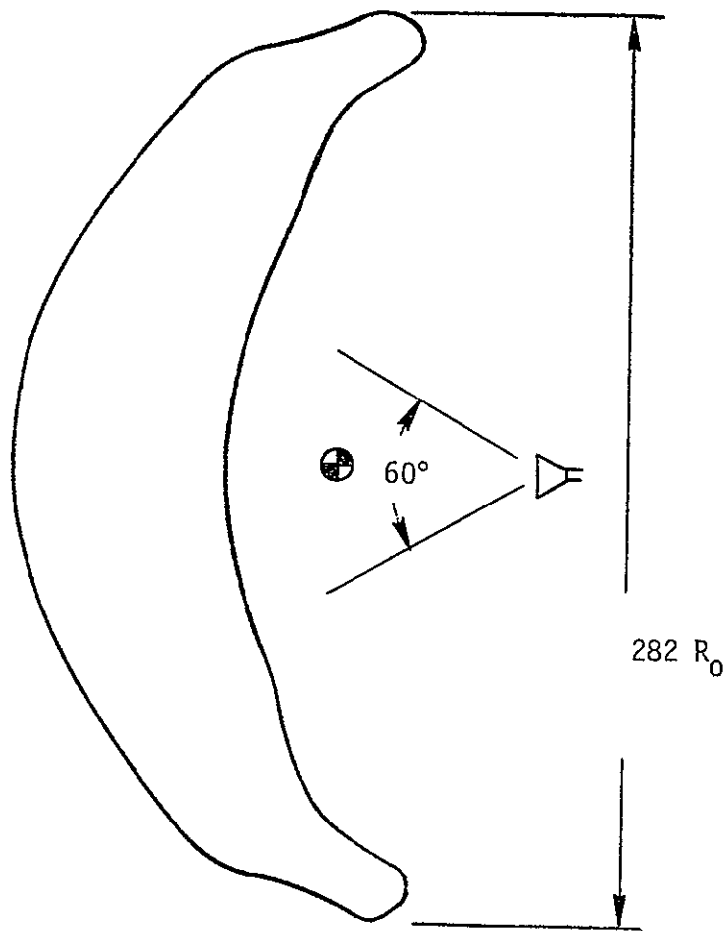


FIG 7 Subreflector configuration

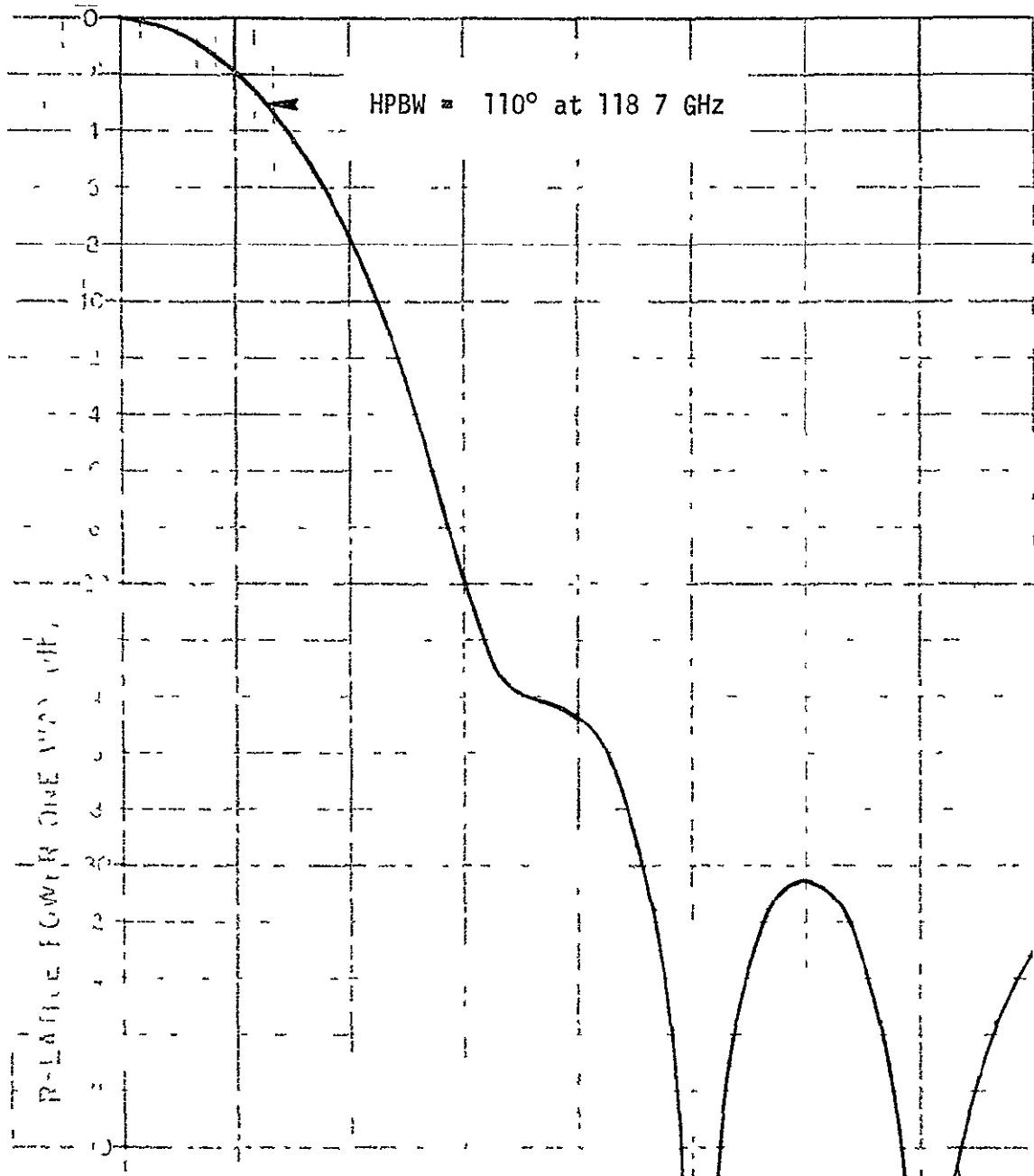


FIG 8 Computed track plane pattern

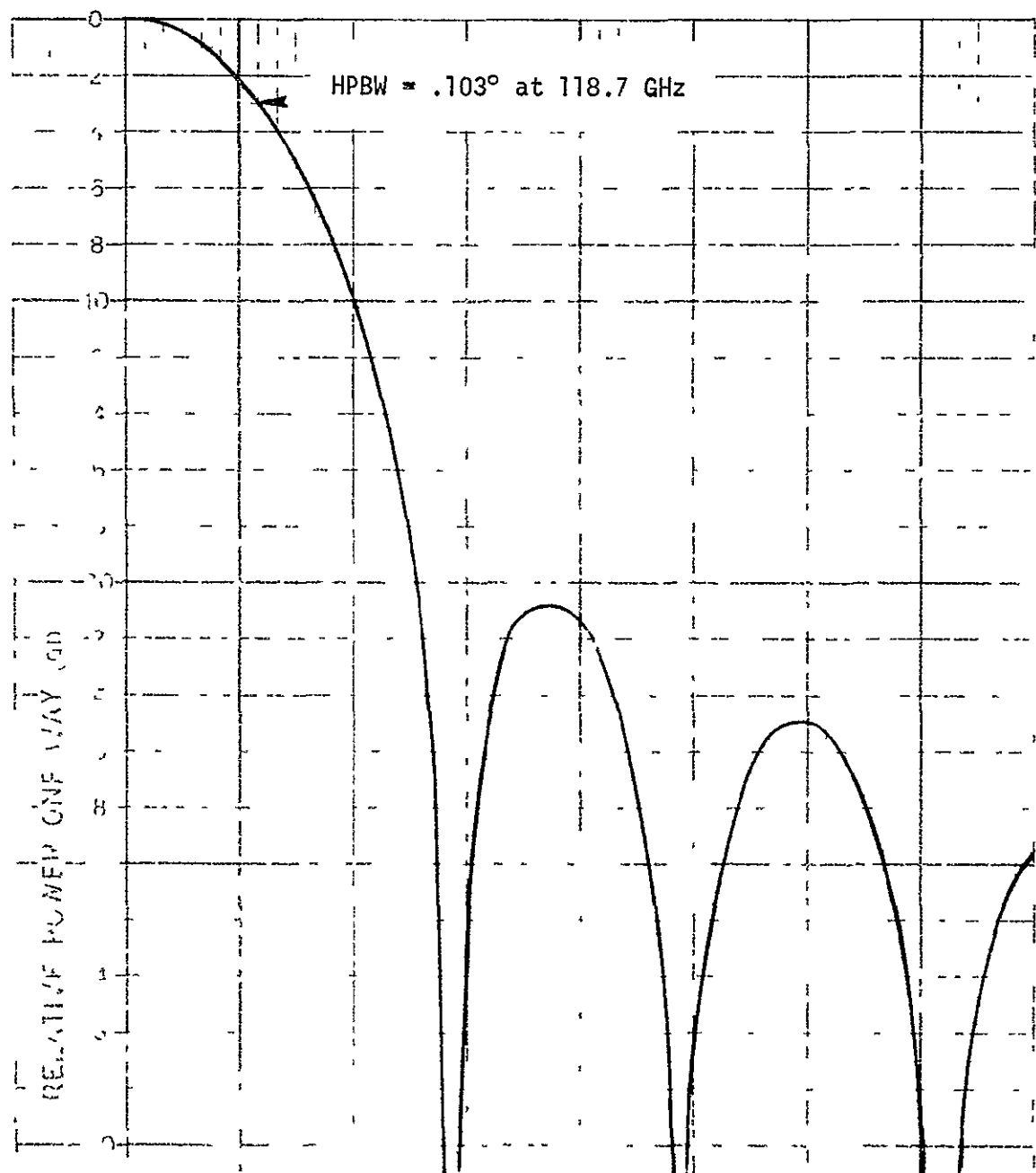


FIG 9 Computed scan plane pattern

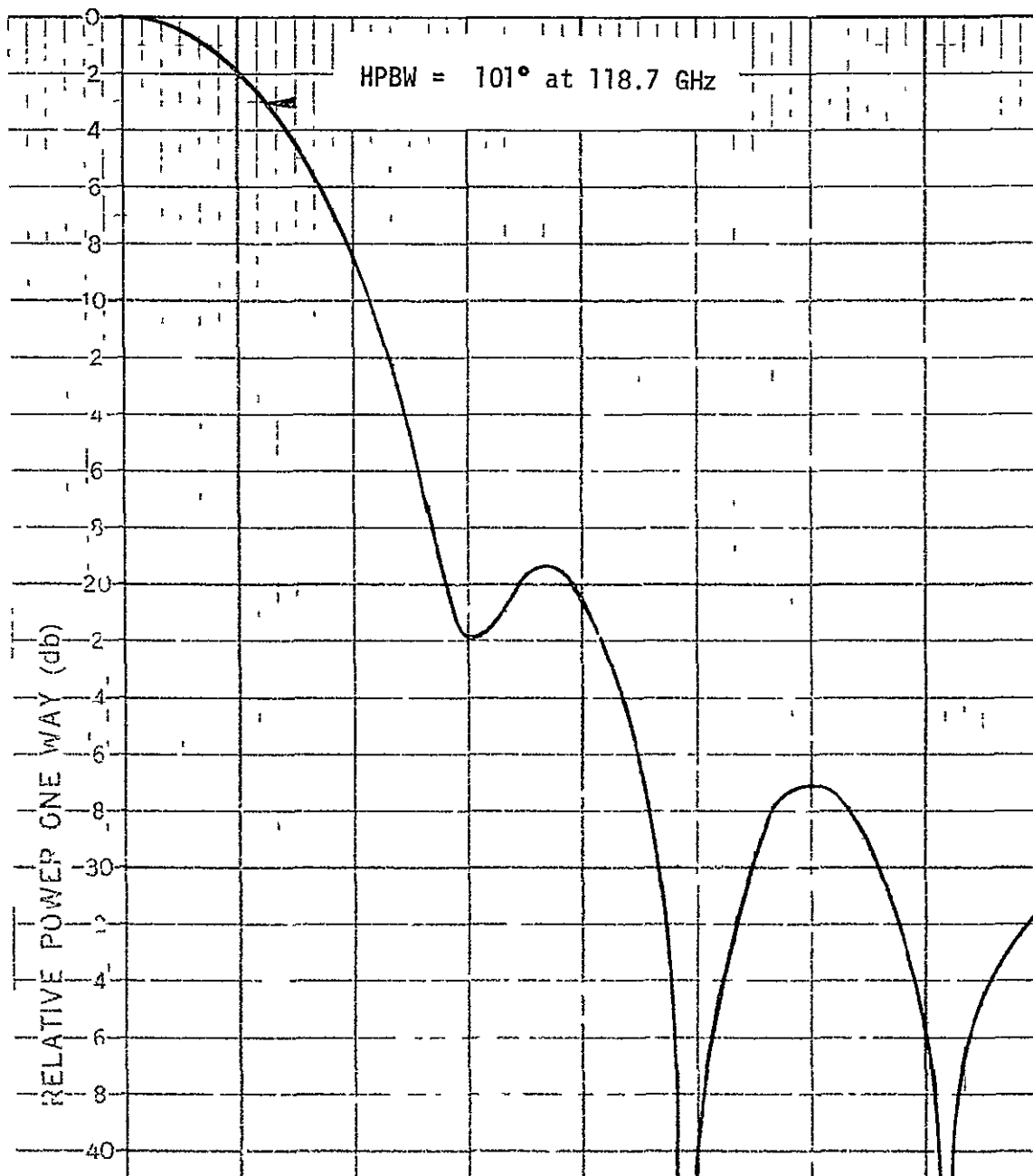


FIG 10 Computed diagonal plane pattern

are of importance. The calculated 3 dB beamwidths for a 2 meter torus radius at 118.7 GHz are shown on the figures and it is seen that these beamwidths are in the order of a tenth of a degree. For a general choice of wavelength and torus radius the beamwidths are given by

$$\begin{array}{ll} \text{Scan Plane} \cdot & \theta = \frac{80^\circ \lambda}{R_0} \\ \text{Diagonal Plane} \cdot & \theta = \frac{82^\circ \lambda}{R_0} \\ \text{Track Plane} & \theta = \frac{87^\circ \lambda}{R_0} \end{array}$$

where θ is the full 3 dB beamwidth and R_0 is the radius of the base of the torus

Antenna patterns were calculated at cut planes every 22.5° around the main beam. These patterns were then integrated numerically to obtain a value for the antenna beam efficiency. It was determined that for the 30° - 60° feed beamwidth choice, 91% of the principally polarized power was contained within a region of full angular width $205^\circ \lambda / R_0$. The well-defined nulls of the antenna pattern in the scan plane fall at the edges of this region. A reduction of the feed-horn beamwidths would result in a higher efficiency pattern with less subreflector spillover but at a cost of wider beamwidths and decreased resolution.

3 0 LOW FREQUENCY STUDY

3 1 Engineering Performance Estimates

The parabolic torus can be fed with simple point source radiators when the frequency is low enough so that the aberration from the torus is negligible. In this section the aperture phase error and cross polarization resulting from the use of such a feed is discussed

3 1 1 Path Length Error

In the analysis of Section 4.2 an expression is developed for the optical path length error $PLE(X,Z)$ at a point X,Z in the aperture plane. This error is representative of the phase error expected at X,Z for a certain point source feed location. The error is expressed as a propagation length normalized to R_0 , the radius of the base of the torus. Fig. 11 shows an aperture map of the type described in Section 2.1. The actual value of the path length error in inches is shown for the case of a point source feed placed directly at the paraxial focal point a distance $R_0/2$ from the base of the torus when $R_0 = 80$ inches. The grid spacing is $(0.1)R_0$ and the dashed circle is the desired 2m diameter radiating aperture. It is seen that the phase length error increases monotonically to a maximum value of about 4.3 inches at the upper right edge of the region to be illuminated. At the lowest frequency of operation, 610 GHz, this would give a maximum phase error estimate of 222 wavelengths at the aperture edge. Such an error would result in quite a small effect on the beam efficiency since the error is relatively small and localized in a region of tapered illumination. Due to the large size of the low frequency feed required at 610 GHz,

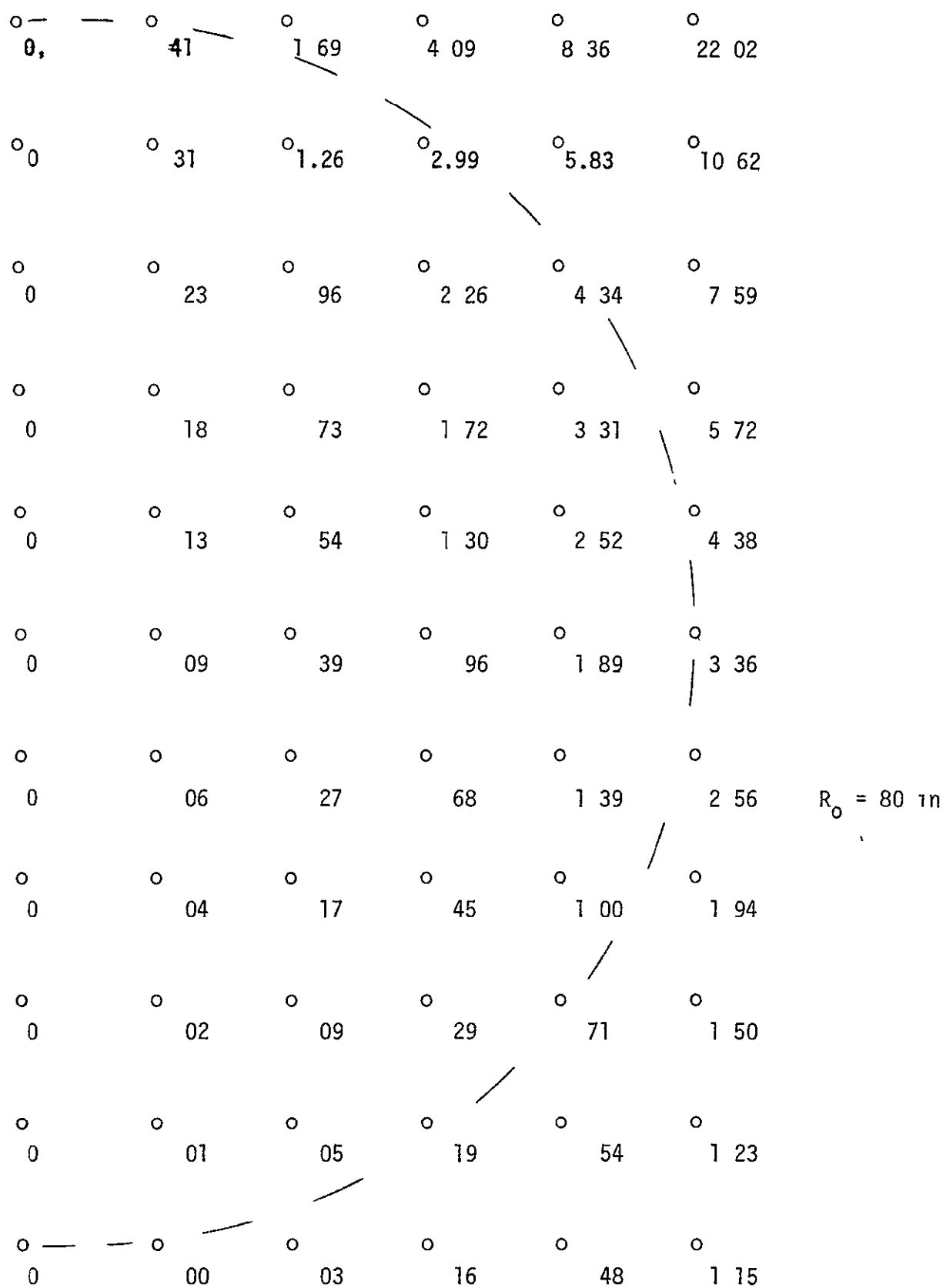


FIG 11 Path length error (in)--feed at paraxial focus

placing the feed at the paraxial focal point results in undesirable blockage. By depressing the feed point a distance $R_0/8$ below the paraxial focus, the feed is completely removed from the radiating aperture. This depression results in an inconsequential 5° squint of the beam up from the plane of the feed wheel.

Actually the paraxial focal point is not the optimum feed position for the minimization of the reflector aberration. The aberration occurs due to the fact that the circular shape of the reflector in one plane has too much curvature. By pushing the feed forward of the paraxial focus the electrical length to the center of the illuminated region is reduced faster than the electrical length to the edges of the illuminated region. This operation has the twofold effect of correcting the aberration and introducing a squint of the antenna beam up from the feed wheel. Fig. 12 shows a map of the path length phase error in inches taking into account a 5.7° beam squint for the case where the feed is located 7.6 inches forward of the paraxial focus and R_0 is 80 inches. Over the entire illuminated region, with the exception of a very small area near the upper right hand edge, the phase error is well under one inch and generally much less than 0.5 inches. From this figure it can be inferred that allowing for the small squint angle a simple point source feed such as a horn or dipole array can be used at least up to 2.695 GHz where the wavelength is 4.38 inches with little regard for the reflector aberration. At 6.6 GHz some feed correction by means of a lens or a polyrod may be required for optimum performance.

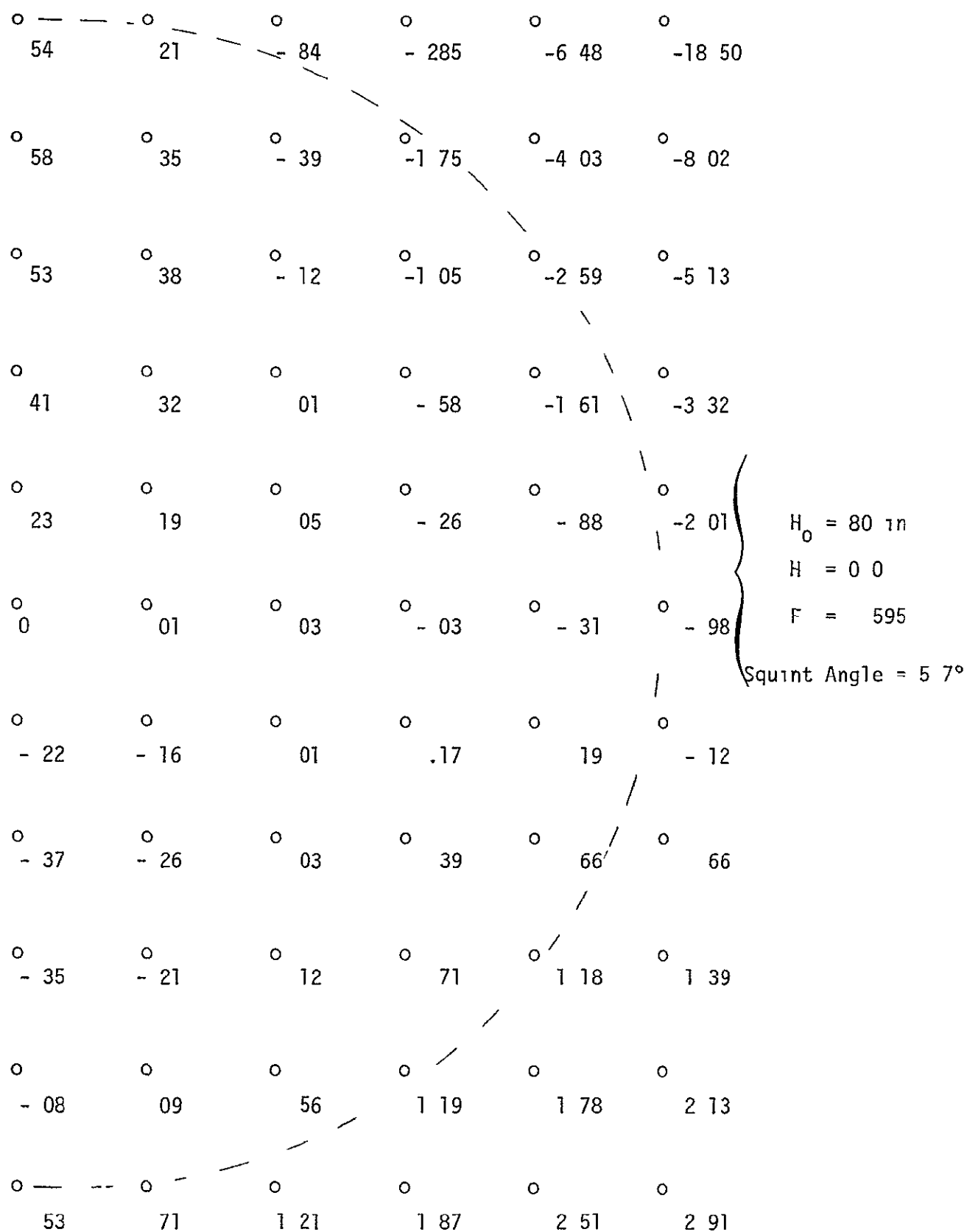


FIG 12 Path length error (in)--feed 7.6 in foward of the paraxial focus

3 1 2 Cross Polarization

In the analysis of Section 4 2 an expression is developed for the principal and cross polarized aperture fields at a point X,Z in the aperture plane. By integrating the square of these fields over the aperture plane, the ratio of total cross polarized power crossing the aperture to the total principally polarized power crossing the aperture was computed. The computations were made for a feed positioned $R_0/8$ below the paraxial focus and pointed up at a 45° angle. Feed 3 dB beamwidths of 45° were assumed in both planes. This arrangement more or less corresponds to the model configuration and the 610 GHz feed configuration in the full size antenna. The integrated total cross polarized power ratios were found to be 2.6% for a vertically polarized feed and 4.3% for a horizontally polarized feed.

3 2 Scale Model

3 2 1 Model Description

In order to determine the low frequency behavior of the offset reflector system a working scale model of the antenna was constructed. The model is shown in Fig. 13. For ease of fabrication the diameter of the torus was chosen to be 16 in. This choice yielded a scale factor of 10.688 for a full size torus radius of 2.174m so that a measurement of the model performance at 6.52 GHz would be representative of the full size antenna at 610 GHz. The height of the model torus is 7.642 in. so that the inclusion of a .282 in. thick slab of absorber could be used to cover the top end plate of the antenna to catch feed spillover. This absorber would then reduce the torus height to 7.360 in. which scales to the required 2m height in the full size antenna.

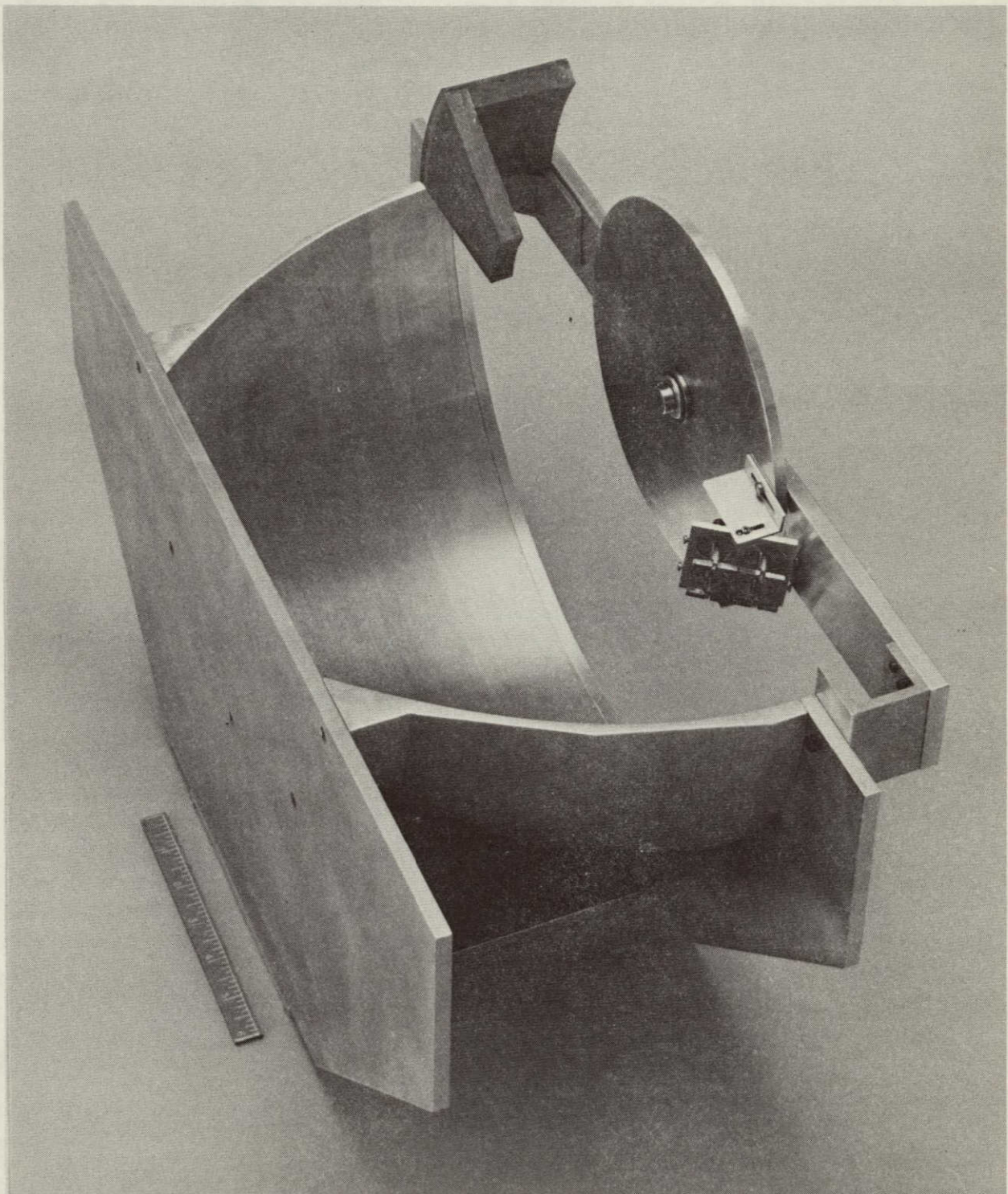


Figure 13. The model antenna.

REPRODUCIBILITY OF THE
ORIGINAL PAGE IS POOR

The reflector was fabricated from a salad bowl shaped aluminum sand casting, cast from a wooden pattern. The casting was machined on a tracer lathe from a template which was cut on a mill with a digital positioning system. The template had an error less than .004 in rms and measurements of the diameters at either end of the reflector indicate that the reflector is also within these tolerance limits. After machining the casting had a minimum wall thickness of 0.2 in and was cut in half to provide the required reflector sector. Before cutting two accurately spaced tooling holes were provided at the reflector edges near the cut lines. After cutting, these holes were then pinned into accurately spaced holes machined into the feed wheel support beam to eliminate the tendency of the cut casting to spring inward at the edges of the cut.

The wooden structure which can be seen in Fig. 13, attached to the feed support wheel is a facsimile of a feed calibration enclosure provided for conceptual purposes. This structure was not present during the model measurements.

3.2.2 Model Feed

The feed for the model antenna can be seen in Fig. 13. This feed consists of an equally spaced array of four dipole radiators. The array elements are half wave spaced at 6.52 GHz with a spacing of .900 in. The ground plane is 2 in square and the length of the dipoles is .850 in. The dipoles are fed by the common split balun arrangement which can be seen in the figure. The dipoles were designed with circular bases which fit into circular holes in the ground plane with set screws so that the radiating elements can be turned 90° to provide either polarization. The

input to each dipole consists of an OSM connector and a four-way power divider was used to feed the array with equal line length flexible cable interconnections. For the model measurements described in this report the feed was positioned such that the center of the ground plane was at a 4-in radius from the wheel center and depressed from the lower edge of the torus a distance of 1 in. The feed was pointed up at an angle of 48° .

3.2.3 Model Measurements

Patterns of the model antenna and feed were measured in a 40 ft anechoic chamber at JPL. The antenna was mounted and the feed wheel turned so that the feed pointed out away from the torus reflector. The radiation patterns of the feed were then measured while it was mounted on the antenna in this fashion. These feed patterns are shown in Fig. 14 and 15. The patterns are not completely smooth, but contain some small ripple structure due to reflections from the torus, supports and antenna mount. In spite of these anomalies it can be seen that the feed patterns are well shaped with an E-plane 10 dB beamwidth of 83° , and an H-plane 10 dB beamwidth of 92° .

The secondary patterns of the antenna were measured for the case of vertical polarization (polarization parallel to the axis of the feed wheel) and with the feed illuminating the central portion of the reflector. The end plate of the antenna was covered with absorber as well as the region directly below the feed wheel in order to catch the feed spillover. Removal of the absorbing material from the antenna increased the spurious energy slightly in the E-plane at regions near 60° of the main beam axis at levels greater than 25 dB down.

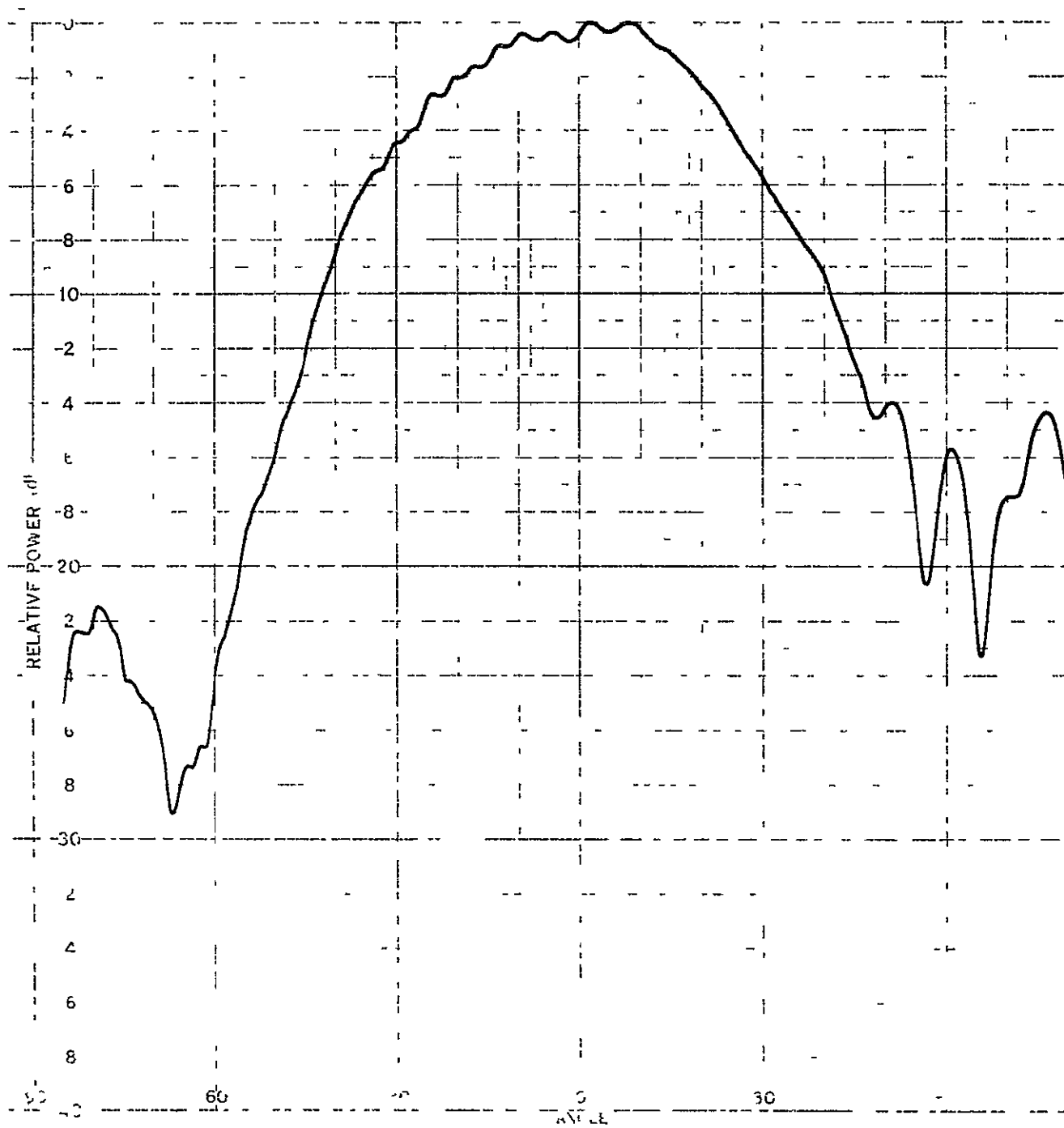


FIG 14 E-plane pattern of the feed array

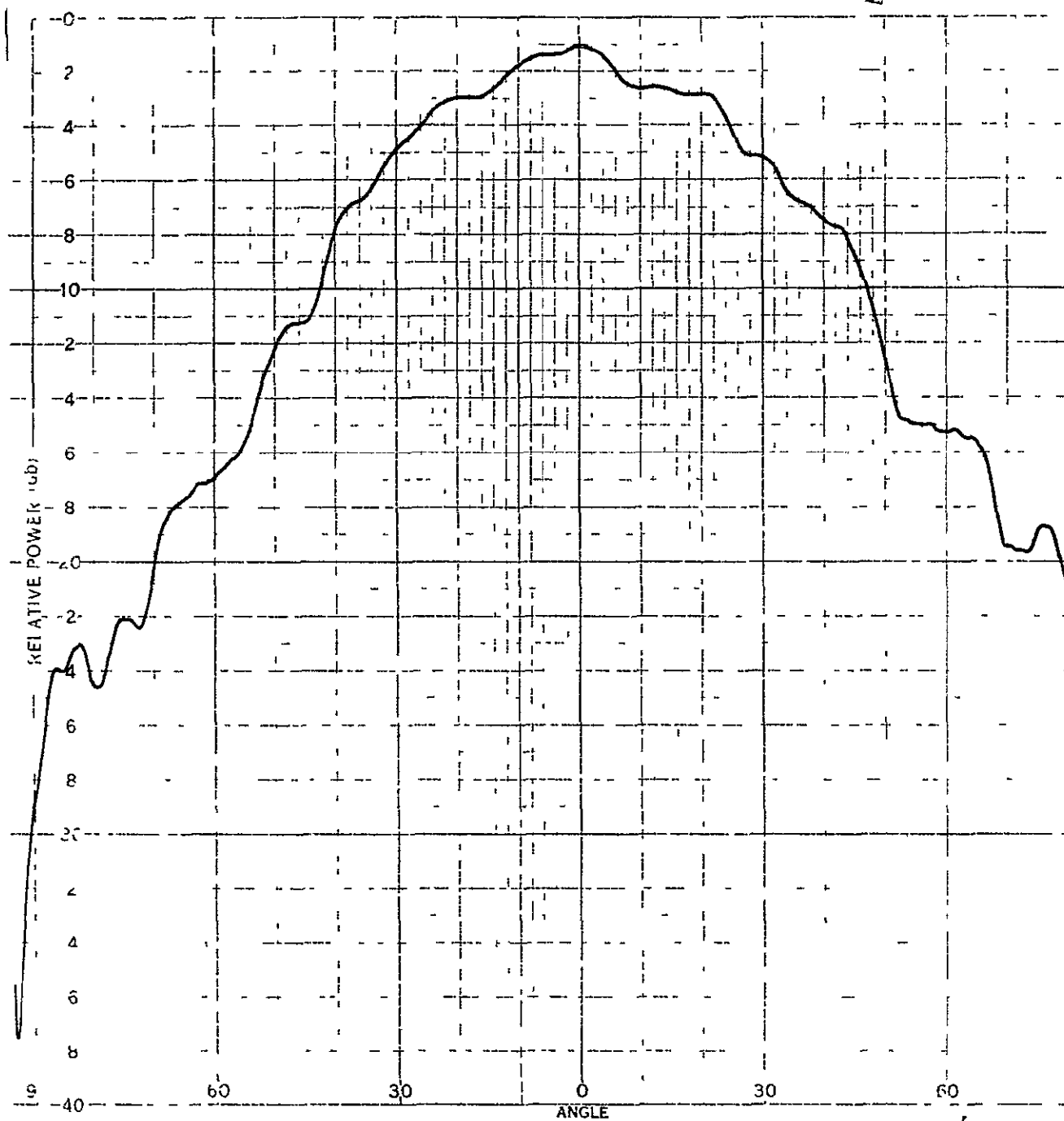


FIG 15 H-plane pattern of the feed array

The antenna secondary pattern for the principal and diagonal planes are shown in Figs 16, 17 and 18. The dashed patterns are those of the cross polarized energy. As can be seen from the figures the principally polarized antenna patterns are excellent with very little energy excluded from the main beam region. The measured antenna 3 dB widths are 16° for the H-plane, 18° for the diagonal plane and 19° for the E-plane cut. The cross polarization levels are generally 20 dB down with the exception of a narrow -14 dB lobe in the plane of the feed wheel. The antenna patterns were integrated numerically and averaged so as to give an estimate of the total antenna beam efficiency. The percentage of the total principally polarized power contained within θ of the main beam axis thus obtained is shown as a function of θ in Fig 19. From the figure it is seen that 95% of the power is contained within 22° of the main beam axis. It should be pointed out that the nulls of the main beam occur at 22° off axis in the diagonal plane where the beam is the narrowest. Also, a reasonably tapered circular aperture with a full 3 dB beamwidth of 18° will have nulls positioned at angles equal to or greater than 22° off axis.

The cross-polarized antenna patterns were also integrated and the total cross polarized power was found to be 3.8% of the total principally polarized power. The majority of cross polarized power is also contained within 22° of the main beam axis. Including the cross polarization loss of approximately 4%, and the principally polarized beam efficiency of 95%, it is seen that 91% of the total radiated power is contained within 22° of the main beam axis.

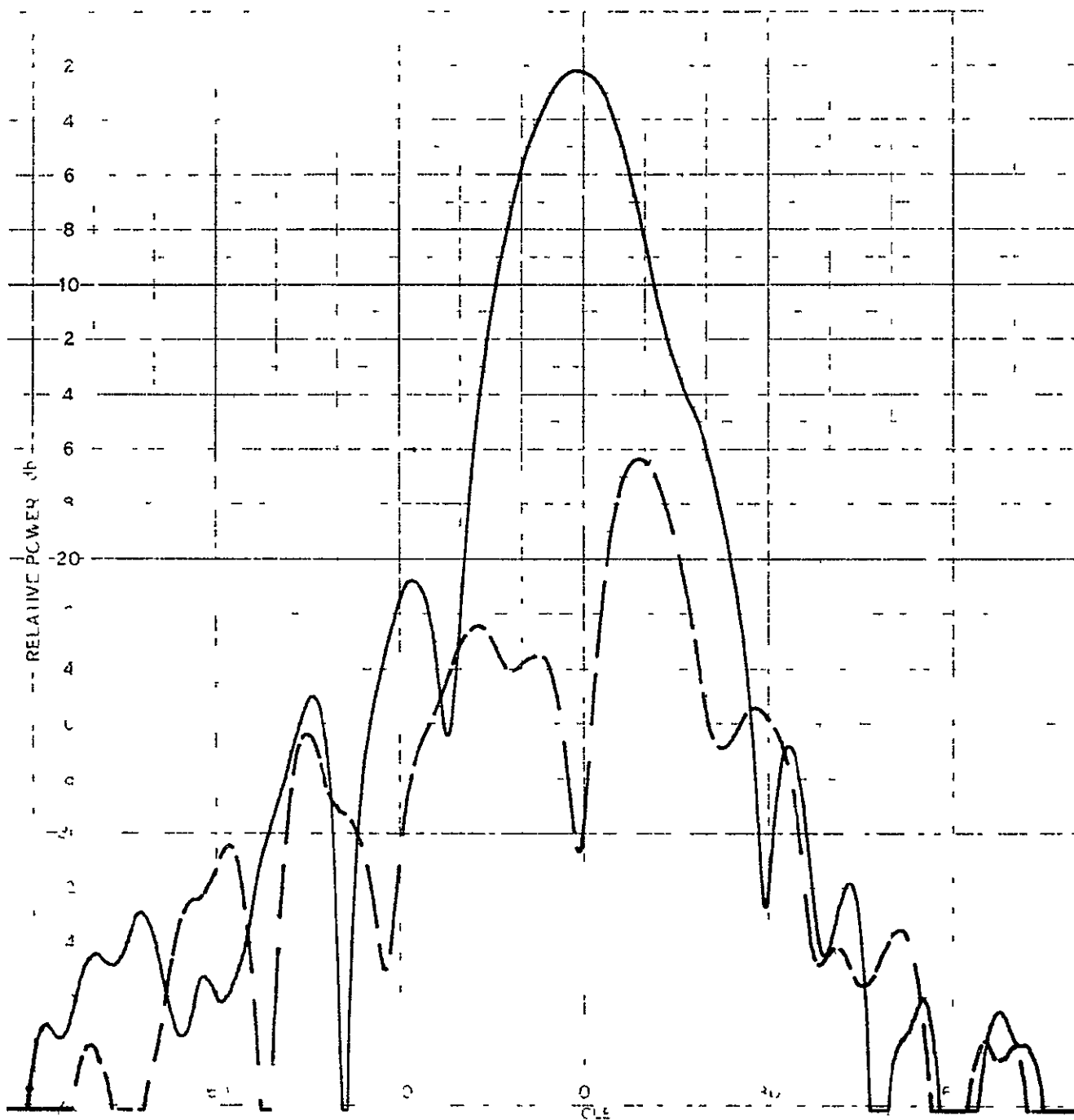


FIG 16 Scan plane (H-plane) secondary patterns for the principal and cross polarizations

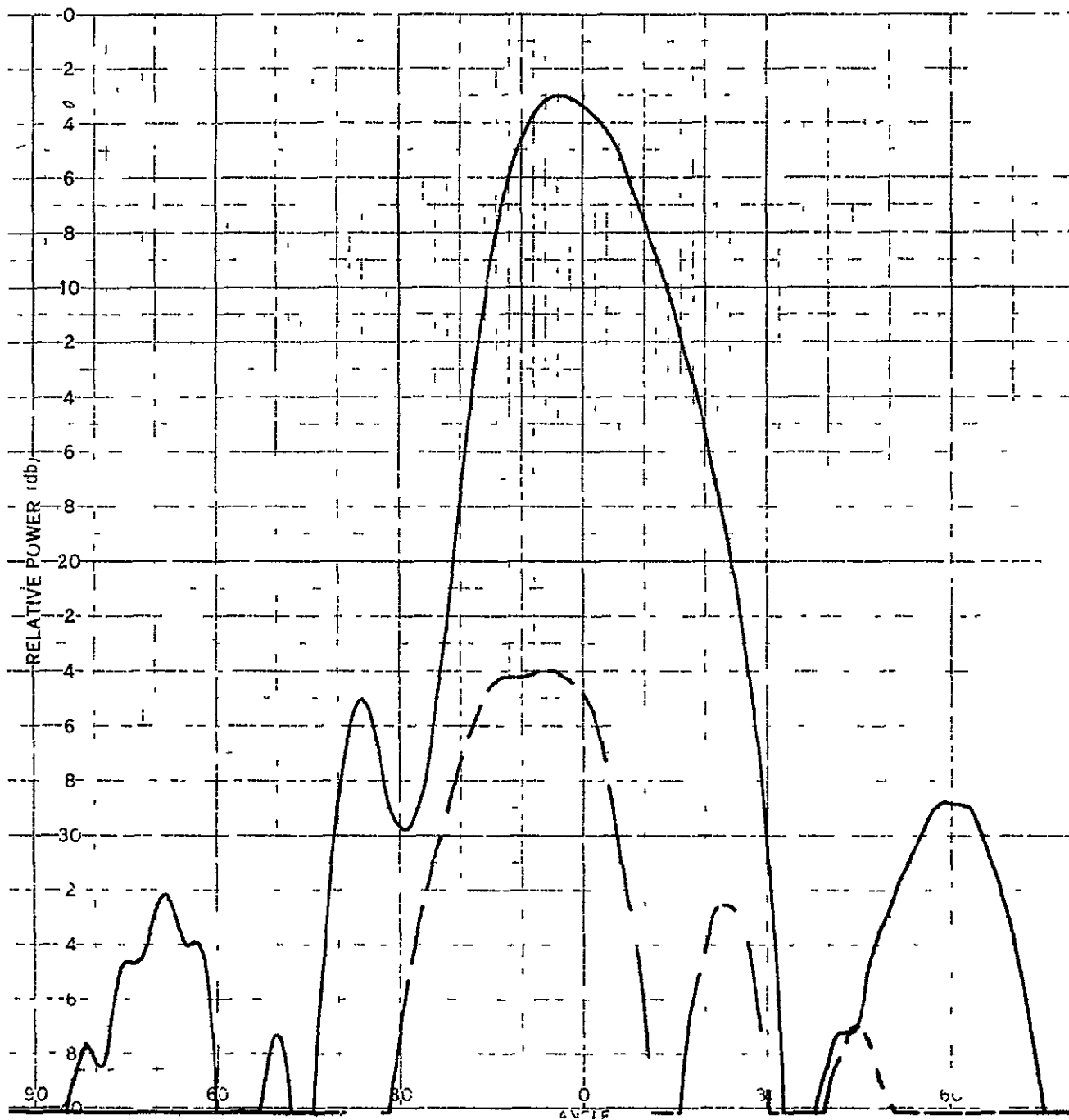


FIG 17 Track plane (E-plane) secondary patterns for the principal and cross polarizations

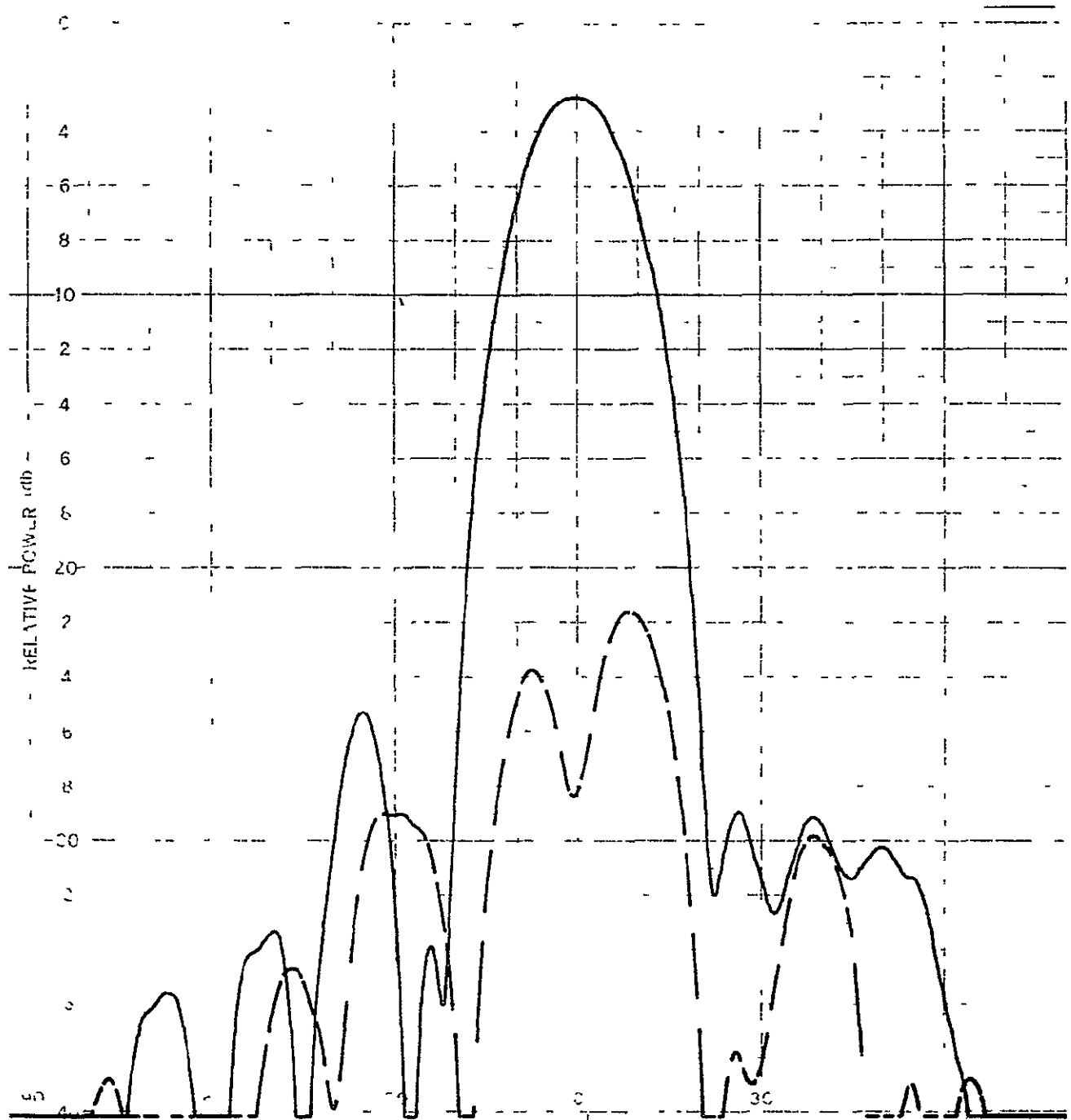


FIG 18 Diagonal plane secondary pattern for the principal and cross polarizations

PERCENTAGE OF TOTAL PRINCIPALLY POLARIZED POWER CONTAINED WITHIN
 θ OF THE MAIN BEAM AXIS

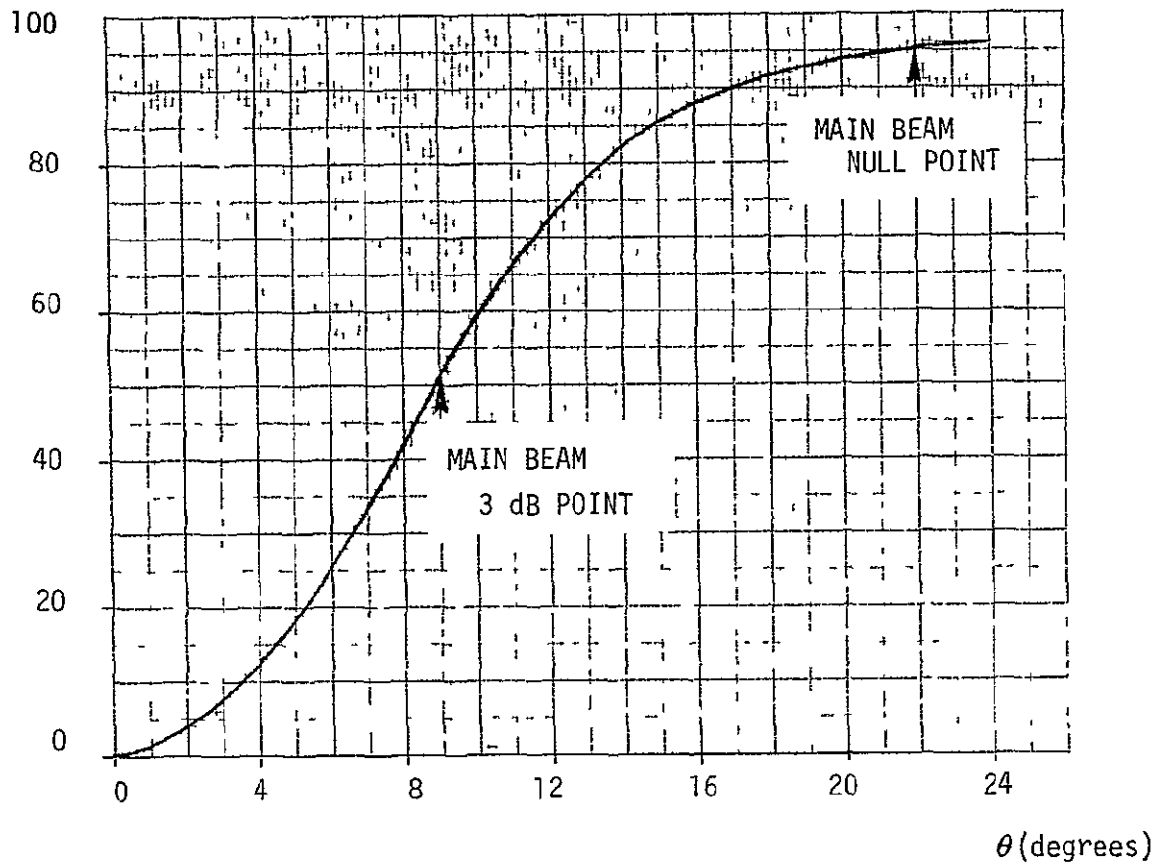


FIG 19 Measured beam efficiency characteristics of the model antenna

4 0 ANALYSES

4.1 Geometrical Optics Analysis

In this section the analysis leading to the computer program describing the high frequency antenna performance is developed. The geometry of the torus, subreflector and feed horn are shown in Fig. 20. To simplify the analysis all distances are normalized to the radius of the bottom of the torus reflector as shown. The analysis is performed with the final objective of a FORTRAN computer program and therefore, an extensive use of FORTRAN type variable names are introduced directly into the algebra of the analysis.

As seen in Fig. 20, the top of the subreflector is located a distance S from the Z -axis which is also the axis of the feed wheel. The X - Z plane is the radiating aperture plane of the antenna. The feed horn is located at the focus of the subreflector a distance F from the Z -axis and a distance H below the top of the subreflector and the bottom of the torus. The paraxial focus of the torus is located a distance 0.5 from the Z -axis. A second coordinate system XX, YY, ZZ is arranged at the subreflector focus in order to describe the coordinates of the subreflector. The objective of the analysis is as follows: given a point X, Z in the antenna aperture plane, and a specification of the design parameters of Table II,

TABLE II
Antenna Design Parameters

F	= Distance of feed horn from wheel axis
H	= Distance of feed horn from bottom of torus
S	= Distance of subreflector top from wheel axis
A	= Feed pointing angle (acute) up from XX - YY plane (degrees)

AZBW = Azimuth 3 dB beamwidth of feed (degrees)

ELBW = Elevation 3 dB beamwidth of feed (degrees)

determine the characteristic quantities listed in Table III. Again, all distances are normalized to the radius of the bottom of the torus

TABLE III

Determined Antenna Characteristics

XX,YY,ZZ	= Coordinates of the point on the subreflector relative to the feed horn on which the ray passing through X,Z impinges
Y	= Coordinate of the point on the torus on which the ray passing through X,Z impinges
G	= Gain of the feed in the direction of the ray from the feed horn to XX,YY,ZZ normalized to unity at the peak of the feed pattern
T	= The ratio of the power per unit solid angle incident at XX,YY,ZZ from an isotropic radiator at the feed position to the power per unit area transported to X,Z
EHC	= Cross polarized aperture field at X,Z for a horizontally polarized feed
EHP	= Principally polarized aperture field at X,Z for a horizontally polarized feed
EVC	= Principally polarized aperture field at X,Z for a vertically polarized feed
EVP	= Principally polarized aperture field at X,Z for a vertically polarized feed
CPRH= EHC/EHP	= Cross polarization ratio for a horizontally polarized feed
CPRV = EVC/EVP	= Cross polarization ratio for a vertically polarized feed

The quantities in Table III will now be determined with sufficient detail to allow their direct implementation in a FORTRAN computer program

TORUS COORDINATES

For a point X and Z in the antenna aperture the projected point on the parabolic torus has a Y-coordinate given by

$$Y = \sqrt{\left(1 - \frac{Z^2}{2}\right)^2 - X^2} \quad (1)$$

SURFACE NORMAL

The parabolic torus is defined by the equation

$$f(X,Y,Z) = \sqrt{X^2 + Y^2} + \frac{Z^2}{2} = 1$$

The surface normal is in the direction of the negative gradient of this function or

$$-\text{grad } f = -X \sqrt{X^2 + Y^2} \vec{a}_x - Y \sqrt{X^2 + Y^2} \vec{a}_y - Z \vec{a}_z$$

The magnitude of this vector is

$$|\text{grad } f| = \sqrt{1 + Z^2}$$

Thus, the three components of the surface normal are

$$N_X = \frac{-X}{\sqrt{(1+Z^2)(X^2+Y^2)}} \quad (2)$$

$$N_Y = \frac{-Y}{\sqrt{(1+Z^2)(X^2+Y^2)}} \quad (3)$$

$$N_Z = \frac{-Z}{\sqrt{1+Z^2}} \quad (4)$$

REFLECTED RAY

Upon reflection the component of the incident ray in the direction of the surface normal is reversed. Thus, for an incident ray in the direction \vec{a}_y the direction of the ray scattered from the reflector is given by

$$\vec{M} = \vec{a}_y - 2NY\vec{N}$$

The three components of the ray from the reflector are then given by

$$MX = -2NY \cdot NX \quad (5)$$

$$MY = 1 - 2NY^2 \quad (6)$$

$$MZ = -2NY \cdot NZ \quad (7)$$

SUBREFLECTOR COORDINATES

The vector extending from the subreflector feed to the illuminated point on the torus is given by

$$\vec{RF} = X \vec{a}_x + (Y-F) \vec{a}_y + (Z+H) \vec{a}_z \quad (8)$$

The vector from the feed to the illuminated point on the subreflector is given by

$$\vec{RR} = -XX \vec{a}_x - YY \vec{a}_y + ZZ \vec{a}_z \quad (9)$$

From the geometry it is clear that

$$\vec{RR} = \vec{RF} + \vec{M} C(X,Z) \quad (10)$$

For phase coherence the scalar function $C(X,Z)$ must be such that

$$Y + C + |\vec{RR}| = \text{constant} = K \quad (11)$$

where K is the total path length from the feed to the X-Z plane

$$K = \sqrt{H^2 + (F-S)^2} + 2 - S \quad (12)$$

From Eqs (10) and (11),

$$|\vec{RR}|^2 = (K-Y)^2 - 2C(K-Y) + C^2$$

$$|\vec{RR}|^2 = |\vec{RF}|^2 + 2C \vec{M} \cdot \vec{RF} + C^2$$

which can be solved to yield

$$C(X,Z) = \frac{(K-Y)^2 - X^2 - (Y-F)^2 - (Z+H)^2}{2[K - Y + MX*X + MY*(Y-F) + MZ*(Z+H)]}$$

and the reflector coordinates are then given by Eqs (10), (12) and (13) as follows

$$XX = -X - C*MX \quad (14)$$

$$YY = F - Y - C*MY \quad (15)$$

$$ZZ = Z + H + C*MZ \quad (16)$$

FEED RAY UNIT VECTOR

The unit vector extending from the feed to the illuminated point on the subreflector is given by

$$\vec{AR} = \vec{RR}/|\vec{RR}| = \vec{RR}/(K - C - Y)$$

Thus, the three components of this vector are

$$ARX = -XX/(K-C-Y) \quad (17)$$

$$ARY = -YY/(K-C-Y) \quad (18)$$

$$ARZ = ZZ/(K-C-Y) \quad (19)$$

COORDINATE DERIVATIVES

It is necessary to compute the following partial derivatives

$$\vec{B} = \frac{\partial \vec{RR}}{\partial X} \quad (20)$$

$$\vec{D} = \frac{\partial \vec{RR}}{\partial Z} \quad (21)$$

This is accomplished by the following INITIAL procedure

Replace X by X + 01	X = X + 01
Compute \vec{RR} and store in B	BX = -XX BY = -YY BZ = ZZ
Return X to its first value	X = X - 01
Replace Z by Z + 01	Z = Z + 01
Compute \vec{RR} and store in D	DX = -XX DY = -YY DZ = ZZ
Return Z to its first value	Z = Z - 01

Compute \vec{RR} then the components of B and D are given by

$$BX = 100*(BX + XX) \quad (22)$$

$$BY = 100*(BY + YY) \quad (23)$$

$$BZ = 100*(BZ - ZZ) \quad (24)$$

$$DX = 100*(DX + XX) \quad (25)$$

$$DY = 100*(DY + YY) \quad (26)$$

$$DZ = 100*(DZ - ZZ) \quad (27)$$

CROSS POLARIZATION RATIO

The subreflector surface normal at the illuminated point is proportional to the vector

$$\vec{U} = \vec{M} + \vec{AR}$$

which has components

$$U_X = M_X + AR_X \quad (28)$$

$$U_Y = M_Y + AR_Y \quad (29)$$

$$U_Z = M_Z + AR_Z \quad (30)$$

For horizontal polarization the magnetic field from the feed is in the direction of the vector

$$\vec{P} = \vec{AR} \times \vec{a}_x$$

which has components

$$P_Y = AR_Z \quad (31)$$

$$P_Z = -AR_Y \quad (32)$$

For vertical polarization the magnetic field from the feed is in the direction of the vector

$$\vec{Q} = \vec{AR} \times (\vec{a}_z \cos A + \vec{a}_y \sin A)$$

where A is the angle at which the feed is tilted up from the horizontal

This vector has components

$$Q_X = AR_Y \cos A - AR_Z \sin A \quad (33)$$

$$Q_Y = -AR_X \cos A \quad (34)$$

$$Q_Z = AR_X \sin A \quad (35)$$

For horizontal polarization the induced subreflector current is then proportional to

$$\vec{JP} = \vec{U} \times \vec{P}$$

which has components

$$JPX = UY*PZ - UZ*PY \quad (36)$$

$$JPY = \quad \quad \quad - UX*PZ \quad (37)$$

$$JPZ = UX*PY \quad (38)$$

For vertical polarization the current is proportional to

$$\vec{JQ} = \vec{U} \times \vec{Q}$$

which has components

$$JQX = UY*QZ - UZ*QY \quad (39)$$

$$JQY = UZ*QX - UX*QZ \quad (40)$$

$$JQZ = UX*QY - UY*QX \quad (41)$$

for horizontal polarization the magnetic field incident on the torus is then proportional to

$$\vec{HH} = \vec{M} \times \vec{JP}$$

which has components

$$HHX = MY*JPZ - MZ*JPY \quad (42)$$

$$HHY = MZ*JPX - MX*JPZ \quad (43)$$

$$HHZ = MX*JPY - MY*JPX \quad (44)$$

For vertical polarization the magnetic field incident on the torus is then proportional to

$$\vec{HV} = \vec{M} \times \vec{JQ}$$

which has components

$$HVX = MY*JQZ - MZ*JQY \quad (45)$$

$$HVV = MZ*JQX - MX*JQZ \quad (46)$$

$$HVZ = MX*JQY - MY*JQX \quad (47)$$

For horizontal polarization the ratio of cross polarized
torus current to principally polarized current is

$$\text{CPRH} = (\vec{N} \times \vec{HH}) \cdot \vec{a}_z / (\vec{N} \times \vec{HH}) \cdot \vec{a}_x$$

which is given by

$$\text{CPRH} = (\text{NX*HHY} - \text{NY*HHX}) / (\text{NY*HHZ} - \text{NZ*HHY}) \quad (48)$$

For vertical polarization the cross polarization ratio is

$$\text{CPRV} = (\vec{N} \times \vec{HV}) \cdot \vec{a}_x / (\vec{N} \times \vec{HV}) \cdot \vec{a}_z$$

which is given by

$$\text{CPRV} = (\text{NY*HVZ} - \text{NZ*HVV}) / (\text{NX*HVV} - \text{NY*HVX}) \quad (49)$$

PRIMARY FEED PATTERN

The component of \vec{AR} along the vertical axis of the feed
aperture is

$$\vec{AR} (\vec{a}_z \cos A - \vec{a}_y \sin A)$$

The component of \vec{AR} along the horizontal axis of the feed aperture is

$$\vec{AR} \vec{a}_x$$

Assuming a Gaussian feed pattern, the feed gain in the direction of AR is given by

$$G = \exp -(\ln 2) \left(\left(\frac{ARX}{\sin(AZBW/2)} \right)^2 + \left(\frac{ARZ \cos A + ARY \sin A}{\sin(ELBW/2)} \right)^2 \right) \quad (50)$$

where AZBW and ELBW are the respective azimuth and elevation full 3 dB beamwidths of the feed

POWER DENSITY TRANSFORMATION

The amount of power crossing an area element $dX dZ$ of the radiating aperture is given by

$$dP = G T dX dZ \quad (51)$$

where G is the gain of the feed pattern in the direction of \vec{AR} and T is the aperture power density per power density per unit solid angle of feed radiation and is given by

$$T = (\vec{B} \times \vec{D} \cdot \vec{AR}) / |\vec{RR}|^2 \quad (52)$$

where B and D are the partial derivatives of \vec{RR} with respect to X and Z , respectively This transformation is given by

$$T = \left(\left| \begin{array}{l} ARX(BY \cdot DZ - BZ \cdot DY) + ARY(BZ \cdot DX - BX \cdot DZ) \\ + ARZ(BX \cdot DY - BY \cdot DX) \end{array} \right| \right) / (K - C - Y)^2 \quad (53)$$

APERTURE FIELDS

For horizontal polarization the total power contained in the principle polarization aperture field EHP and the cross polarized aperture field EHC is given by

$$EHP^2 + EHC^2 = EHP^2(1 + CPRH^2) = G \cdot T$$

so that

$$EHP = \sqrt{G \cdot T / (1 + CPRH^2)} \quad (54)$$

$$EHC = CPRH \cdot EHP \quad (55)$$

Similarly for vertical polarization

$$EVP = \sqrt{G \cdot T / (1 + CPRV^2)}$$
$$EVC = CPRV \cdot EVP \quad (57)$$

4 2 Low Frequency Analysis

In this section the analysis describing the engineering estimates of the low frequency antenna characteristics will be given. For the sake of convenience the geometry will be chosen identical to that of the high frequency analysis as illustrated in Fig 20. In this case the feed is still located at the point O,F,-H, but is turned around so that it illuminates the reflector directly and of course the subreflector is removed. Again, the feed points up through an acute angle A from the X-Y plane. All distances are again normalized to the torus radius. The quantities F,H,A,AZBW,ELBW,EHC,EHP,EVC,EVP,CPRH and CPRV remain as defined in Tables II and III. The objective of the low frequency

analysis is as follows Given a point X, Z in the antenna aperture plane and a specification of F, H and A determine the principally polarized aperture fields EHP, EVP, cross polarization ratios CPRH, CPRV and the path length error PLE PLE is the path length along a ray extending from the feed to the point X, Y, Z on the reflector and then to the point X, Z in the aperture plane minus the value of a similar path length for the ray extending from the feed to the point $0, 1, 0$ on the reflector and then to the point $0, 0$ in the aperture plane PLE is a measure of the phase error occurring at X, Z due to the aberrations experienced by a point source feed The error defined in this way is normalized to zero at the point $0, 0$ in the aperture

PATH LENGTH ERROR

The path length from the feed to the point X, Y, Z on the reflector is simply

$$\sqrt{(Y-F)^2 + (Z+H)^2 + X^2}$$

where Y is given by (1)

The path length from the point X, Y, Z to the point X, Z in the aperture plane is Y and therefore

$$\begin{aligned} \text{PLE} = & \sqrt{(Y-F)^2 + (Z+H)^2 + X^2} + Y \\ & - \left[\sqrt{(1-F)^2 + H^2} + 1 \right] \end{aligned} \quad (58)$$

CROSS POLARIZATION

Let the vector extending from the feed at $0, F, -H$ to the point X, Y, Z be \vec{L}

$$\vec{L} = X \vec{a}_x + (Y-F) \vec{a}_y + (Z+H) \vec{a}_z \quad (59)$$

For horizontal polarization the incident magnetic field impinging on X, Y, Z is in the direction $\vec{L} \times \vec{a}_x$ and thus the surface current density will be proportional to

$$\vec{J}(X, Y, Z) = \vec{N} \times (\vec{L} \times \vec{a}_x)$$

where N is the surface normal given by (3), (4) and (5) Assuming the aperture fields are proportional to the projection of the surface current the cross polarization ratio is then

$$CPRH = \frac{J_z}{J_x} = \frac{-X (Z+H)}{Y(Y-F) + Z(Z+H)\sqrt{X^2+Y^2}} \quad (60)$$

For vertical polarization the magnetic field from the feed is in the direction of the vector

$$\vec{Q} = \vec{L} \times (-\vec{a}_y \sin A + \vec{a}_z \cos A)$$

and the induced surface current is proportional to

$$\vec{J} = \vec{N} \times \vec{Q}$$

The cross polarization ratio is then given by

$$CPRV = \frac{J_x}{J_z} = \frac{-X (-Y \sin A + Z \sqrt{X^2+Y^2} \cos A)}{Y(Z+H) \sin A + X^2 \cos A + Y(Y-F) \cos A} \quad (61)$$

APERTURE FIELDS

The unit vector \vec{AL} pointing from the feed point $O, F, -H$ to the illuminated point at X, Y, Z is

$$\vec{AL} = \vec{L}/|\vec{L}| = ALX \vec{a}_x + ALY \vec{a}_y + ALZ \vec{a}_z$$

For a feed pointing up at an angle A from the horizontal the component of \vec{AL} along the vertical axis of the feed is then

$$\vec{AL} (\vec{a}_z \cos A - \vec{a}_y \sin A)$$

The component of \vec{AL} along the horizontal axis of the feed is

$$\vec{AL} \cdot \vec{a}_x$$

Assuming a Gaussian feed pattern, the feed gain in the direction of \vec{AL} is given by

$$G_f(\vec{L}) = \exp -(\ln 2) \left(\left(ALX/\sin (AZBW/2) \right)^2 + \left((ALZ \cos A - ALY \sin A)/\sin (ELBW/2) \right)^2 \right) \quad (62)$$

Since the energy is collimated as it leaves the reflector the energy density in the aperture is identical to the energy incident at X, Y, Z . Taking into account the $|\vec{L}|^{-2}$ space attenuation and the fraction of the power appearing as cross polarization, the principally polarized fields at X, Z in the aperture are proportional to

$$EHP = \sqrt{G(\vec{L})/(1+CPRH^2)} \cdot |\vec{L}|^2 \quad (63)$$

and

$$EVP = \sqrt{G(\vec{L})/(1+CPRV^2)} \cdot |\vec{L}|^2 \quad (64)$$

The cross polarized fields at X,Z are given by

$$E_{HC} = C_{PRH} \cdot E_{HP} \quad (65)$$

and

$$E_{VP} = C_{PRV} \cdot E_{VP} \quad (66)$$

5 0 CONCLUSIONS AND RECOMMENDATIONS

In view of the study results summarized in Section 1 3 it is concluded that the offset fed parabolic torus is a viable solution to the problem of meeting the SIMS antenna requirements. The work described in this report verifies that acceptable antenna performance is possible at the high and low ends of the required frequency range.

It is recommended that further study be performed in the middle frequency range at 6.6 and 10.69 GHz, where the low frequency feeds begin to require aberration correction and the high frequency optical analyses begin to fail. The objectives of this work would be to determine how low in frequency the subreflectors are useable and the design of an aberration corrector for use with the point source feeds in this transition region.

It is also recommended that the behavior of the antenna near the limits of the range of scan be investigated in order to determine the optimum choice for the torus radius as discussed in Section 2 2.

6 0 NEW TECHNOLOGY

No reportable items of new technology have been identified in the work described in this report.

7 0 REFERENCES

- 1 Gustinovic, J J , "Spherical Reflector Feasibility Study,"
JPL Contract No 560080, Report No TR 068,
December 20, 1974

8.0 APPENDIX A

```

C PROGRAM MAIN
  NAMELIST/DATA/H,F,S,A,AZBW,ELBW
  NAMELIST/DATA2/XX,YY,ZZ,Y,G,T,CPRH,CPRV,EHP,EHC,EVP,EVC,X,Z
  REAL NX,NY,NZ,MX,MY,MZ,K,JPX,JPY,JPZ,JQA,JQY,JQZ
C DESIGN PARAMETERS OF TABLE II ARE READ IN AT THIS POINT
C WITH THE NAMELIST FORMAT LABELED DATA
  READ(5,DATA)
C INPUT PARAMETERS FROM TABLE II ARE WRITTEN OUT AT THIS POINT
C WITH NAMELIST FORMAT LABELED DATA
  WRITE(6,DATA)
C SPECIFY THE APERTURE COORDINATES X AND Z AT THIS POINT
  X=
  Z=
1  L= 0
  X=X+.01
  GO TO 2
3  BX= -XX
  BY = -YY
  BZ = ZZ
  L = -1
  X = X - .01
  Z = Z + .01
  GO TO 2
4  DX= -XX
  DY = -YY
  DZ = ZZ
  L = 1
  Z = Z - .01
2  Y= SQRT(ABS( (1.-Z**2/2.)*^2 - X**2 ) )
  NZ = SQRT(1.+Z**2)
  NY = SQRT(X**2 + Y**2)
  NX = -X/(NZ*NY)
  NY = -Y/(NZ*NY)
  NZ = -Z/NZ
  MX = -2.*NY*NX
  MY = 1. -2.*NY*NY
  MZ = -2.*NY*NZ
  K = 2. -S + SQRT(M**2 + (F-S)**2 )
  C = .5*((K-Y)**2-X**2-(Y-F)**2-(Z+1)**2)/
  * (K-Y+1/2*X*MX+MY*(1-F+1/2*Z*(Z+1)) ,
  XX = -X - C*MX
  YY = F - Y - C*MY
  ZZ = Z + 1 + C*MZ
  IF (L) 4,3,5
5  BX = 100.*(BX + XX)

```

```

BY = 100.*(BY + YY)
BZ = 100.*(BZ - ZZ)
DX = 100.*(DX + XX)
DY = 100.*(DY + YY)
DZ = 100.*(DZ - ZZ)
ARX = K-C-Y
ARY = -YY/ARX
ARZ = ZZ/ARX
ARX = -XX/ARX
UX = MX + ARX
UY = MY + ARY
UZ = MZ + ARZ
PY = ARZ
PZ = -ARY
QX = ARY*COS(A/57.3) - ARZ*SIN(A/57.3)
QY = -ARX*COS(A/57.3)
QZ = ARX*SIN(A/57.3)
JPX = UY*PZ - UZ*PY
JPY = -UX*PZ
JPZ = UX*PY
JQX = UY*QZ - UZ*QY
JQY = UZ*QX - UX*QZ
JQZ = UX*QY - UY*QX
HHX = MY*JPZ - MZ*JPY
HHY = MZ*JPX - MX*JPZ
HHZ = MX*JPY - MY*JPX
HVX = MY*JQZ - MZ*JQY
HVV = MZ*JQX - MX*JQZ
HVZ = MX*JQY - MY*JQX
CPRH = (NX*HHY-NY*HHX)/(NY*HHZ-NZ*HHY)
CPRV = (NY*HVZ-NZ*HVV)/(NX*HVV-NY*HVX)
G= EXP(-(ALOG(2.))*((ARX/SIN(AZBW/114.6))**2+
* ( (ARZ*COS(A/57.3)+ARY*SIN(A/57.3) )/SIN(ELBW/114.6) )**2 ) )
T= ABS( ARX*(BY*DZ-BZ*DY)+ARY*(BZ*DX-BX*DZ)+ARZ*(BX*DY-BY*DX)
* )/(K-C-Y)**2
EHP = SQRT( G*T/(1.+CPRH**2) )
EHC = CPRH*EHP
FVP = SQRT( G*T/(1.+CPRV**2) )
EVC = CPRV*EVP
C OUTPUT PARAMETERS FROM TABLE III ARE WRITTEN OUT AT THIS POINT
C WITH NAMELIST FORMAT LABELED DATA2
WRITE(6,DATA2)
STOP
END

```